Universidad
Carlos III de Madrid

AEROSPACE ENGINEERING

Academic Year 2014/2015
Bachelor Thesis

COMMERCIAL AIRCRAFT TRAJECTORY OPTIMIZATION USING OPTIMAL CONTROL

Author: Rubén Antón Guijarro
Supervisor teacher: Manuel Soler Arnedo

Abstract

The actual air traffic system, based on way points, airways and procedures, is evolving to a new paradigm. This new system will be based on a greater freedom for the airlines to plan their own trajectories allowing more efficient flights. Progresses in this field will bring reduction in fuel consumption with, not only the corresponding economical savings, but also important improvements against environmental impact.

In order to compute the optimal trajectory, a typical approach is using optimal control theories. The main goal of this project is the optimization of commercial aircraft trajectories using optimal control. Different methods can be applied to solve the optimal control problem and some of them have been used with positive results in flight optimization. In this analysis, it has been applied Legendre pseudospectral method to discretize the problem which has not been so widely used, but has interesting properties as its fast rate of convergence.

The problem definition is joined to a flight plan model which must include multiple elements involved in a flight. Among these elements it must be considered appropriate approaches to the motion of the aircraft with different aerodynamic configurations, the atmosphere, the wind and the corresponding restrictions arising from flight envelope, operational departure and approaching procedures and waypoints.

The discretization of the model using Legendre pseudospectral method converts the infinite-dimensional problem into a finite-dimensional one. This allows the transformation into a Non-Linear Programming (NLP) problem which has been solved iteratively from a starting guess using specific software: AMPL and IPOPT.

By mean of three introductory problems, the methods have been proved. Finally a particular case study which consists in a realistic fuel-optimizing flight from Madrid Barajas to Berlin Schöenefeld has been implemented and the results have been analysed.

Contents

List of Figures

List of Tables

Chapter 1

Introduction

1.1 Motivation

The flight plan optimization is the central concept of the project motivation. The flight plan is a process, prepared in advance to the take-off, which the International Civil Aviation Organization (ICAO) defines as the "Specific information provided to air traffic services units, relative to an intended flight or portion of a flight of an aircraft". Among that specific information it can be found the route to follow, altitude levels, velocity profiles and safety information.

The flight plan, is built in a controlled aerial space and in concordance with the requirements stated by the Air Traffic Control (ATC). The route between departure and arrival airports follows the airways defined between fixed waypoints. The airways can be gone over at different altitude levels. Furthermore, they are restricted to determined velocities. To accomplish the route, the aircraft can change the followed airway at the fixed waypoints, and in some cases the ATC can allow a trajectory between two waypoints even if there does not exist an airway between them. In some transoceanic areas, free flight is allowed.

A route definition involves considering three parts of the flight: departure, en-route and arrival. Departure phase must follow the normalized operations called Standard Instrumented Departure (SID) which try to make this phase a safer operation. Analogously, the approaching phase follows a Standard Terminal Arrival Route (STAR) and a final approach procedure. Nowadays, the calculation of the trajectory as part of the flight plan definition, is carried out in two phases. Firstly, the route in 2D is computed using different

algorithms and after that the velocities and altitudes based on previous empiric knowledge. These techniques provide safe trajectories, but sometimes entail inefficient flights.

Regarding the improvement of the trajectory efficiency, its optimization implies a complete analysis in time and space. This 4D approach can be obtained using optimal control theories which may provide the entire set of optimal parameters (including the attitude angles, velocities, consume, etc.) for a trajectory between two points, as a function of time and subjected to the particular restrictions involved. The variable to minimize might be the fuel consumption, the flight time and also functions of both, costs and others. This leads to not only economical savings but also big improvements against environmental impact.

Despite these theories can be applied to the current air traffic system, the procedures to follow do not allow an enough flexibility for optimization. For this reason, and looking for a general improvement in flight efficiency, the air traffic structure is evolving to a new paradigm (the so-called Trajectory-Based Operations (TBO)) in which airlines will have a greater freedom to define the trajectories matching their business interests. The trajectories defined by the airline, which are the owners of the routes, will be settle together with the Air Traffic Service (ATS) Authorities which will provide safety support. The NexGen and SESAR programs in USA and Europe respectively are facing this future, in which optimization of trajectories will have a central importance.

1.2 Goals

Attending to the motivation of the study, this project faces the commercial aircraft trajectory optimization applying optimal control theory and pseudospectral methods to a complete flight plan model. The main goals can be then described in the following points:

- Review of optimal control theories.
- Review of pseudospectral methods.
- Construction of a realistic flight model in optimal control problem form.
- Review of computational tools to solve the adjoin non-linear programming problem.

1.3 Methodology

This section aims to introduce the way the study has been developed and the steps followed to implement the theories in a case study. In addition, it has been introduced information regarding the state of the art for a better understanding of the matter.

As it has been introduced in the project motivation, improvements in the routes efficiency can be treated by mean of a trajectory optimization problem. A typical way of defining the problem is using optimal control theories.

The theories concerning optimal control can be found in different references ([3], [4] and others). In Chapter 2, it is shown the general definition of an optimal control problem which allow the minimization of a functional subjected to dynamic and algebraic constraints. As it will be explained later, it must be mentioned, just as introduction, that the functional to minimize along the project will be the fuel consumption and the flight plan model will determine the set of constraints.

Different methods can be found to solve the optimal control problem. The three main families are Dynamic Programming (DP), Indirect and Direct methods. Due to the complexity of the problem, in general, no analytical solution is possible to find even for the most simple cases and numerical methods must be applied. The different advantages and drawbacks of the methods are summarized in Section 2.3.

The most suitable approaches to solve this kind of optimal control problems belongs to the last family and are the direct collocation methods. They use numerical approaches to discretize the equations and convert the problem into a Non-Linear Programming (NLP) problem. One of them is the well-known Hermite-Simpson method that uses local discretization and has been already widely used to solve flight optimization problems. This project has studied pseudospectral approaches and specially Legendre psudospectral method, which despite of the fact that pseudospectral methods (PS) have not been so extensively used, they provide a global discretization which can be also applied to solve the flight optimization. Furthermore, important properties of PS methods, as their fast rate of convergence, make them an interesting matter of study.

Pseudospectral methods were originally developed to solve the partial

differential equations that arise in fluid mechanics field. However, they have been already proved as computational methods for solving optimal control problems. In fact over the last 10 years, they have been moved from mathematical theory to real applications. They have allowed solving highly complicated non-linear optimal control problems by advances in algorithms and technologies. One the most interesting examples took place on November 5, 2006 and March 3, 2007 when an attitude manoeuvre of the International Space Station (ISS) was tracked without using propellant generating around US$1.5M savings. A review of the pseudospectral methods theory and its application to the particular problem of the project is gathered in chapter 3.

In order to define the flight plan, the aircraft dynamics and the elements affecting the flight have been faced by the development of a complete model that leads to realistic simulation. The model includes: dynamic non-linear equations of motion, different aerodynamic configurations, Earth and atmosphere models, aircraft model, wind and departure and approaching procedures among others. From this model, different restrictions arise like flight envelope constraints, waypoints, dynamic modes, etc. The complete description of the elements modelled is collected in Chapter 4.

In order to prove the methods, three introductory problems have been solved focusing on specific aspects of the model, and finally, it has been implemented a complete case study collected in Chapters 5 and 6 respectively.

The case study of the project considers the resolution of a fuel optimization problem for a concrete flight plan. The flight chosen has been a route from Madrid Barajas to Berlin Schöenefeld. The problem solved is the same case study developed using Hermite-Simpson method in [11]. However the comparison between both methods is out of the scope of the study. A complete description of the problem is defined in Section 6.2.

For the implementation of the problem AMPL language and IPOPT (as NLP solver) have been used. AMPL [7] is a modelling language for describing and solving large-scale optimization problems and it is one of the most common formats used to represent mathematical programming problems. AMPL is complemented by the possibility of using multiple solvers. The one used in this case (IPOPT), is a software library that allows the optimization of non-linear continuous systems.

1.4 Structure

Below, the different chapters in which this report is divided are collected together with a short description of the information containing.

- **Chapter 2 - Optimal control:** important concepts and general optimal control problem definition. Multiphase approach and review of the different solving methods.
- **Chapter 3 - Pseudospectral methods:** brief description of pseudospectral methods family and deepest analysis of the Legendre pseudospectral method and its application.
- **Chapter 4 - Models:** description of the different approaches to the elements involved in a realistic flight plan. Equations of motion, dynamic modes, operative procedures and constraints, atmosphere and wind models, aircraft model, etc.
- **Chapter 5 - Introductory problems:** three toy problems in order to check model and methods are presented. In addition important results have been solved before facing a complete and realistic flight optimization problem.
- **Chapter 6 - Case study:** solution of a realistic flight optimization problem (route Madrid-Berlin) including all the elements: operative procedures, wind, etc. Analysis of the results from the performance and numerical method point of view.
- **Chapter 7 - Conclusions:** review of the main results obtained and description of the possible future work.

Chapter 2

Optimal control

This section gathers the optimal control theories to be applied to the optimization of flight plans. First of all, the general control problem is described and the notation is detailed. The optimal control problem defines the variable to minimize as a functional, which in the case of this project is the mass of fuel burned. The minimization of this functional is subjected to multiple restrictions, including dynamic, algebraic constraints (equality and inequality). A complete reference of optimal control theory is presented in [3] and [4].

From the solving perspective, three different main approaches can be found to solve optimal control problems: Dynamic Programming (DP), Indirect and Direct methods. Finding an analytical solution for optimal control problems may be an impossible task even for the simple cases. For this reason, typically numerical methods must be applied.

Dynamic programming methods [2] use Hamilton-Jacobi-Bellman equation to derive the optimality conditions, but due to fundamental problems they are useless for such a problem like flight optimization. Indirect methods use Prointryagin's Maximum principle [9] for the optimality conditions derivation. They are easier to handle from theoretical point of view, however, also problems from the sensitivity of the adjoin boundary value problem appear. Direct methods, and specially direct collocation methods, are the family of methods used to avoid the problems associated to the other approaches. Direct collocation methods include different numerical approaches as Hermite-Legendre-Gauss-Lobatto and pseudospectral methods.

A brief review of the different solving approaches is developed in the last section of this chapter: Section 2.3, where the main characteristics of the methods are discussed (including advantages and drawbacks). A deeper analysis of pseudospectral theories and specially of Legendre pseudospectral method is collected in Chapter 3.

2.1 General optimal control problem

The General Optimal Control Problem [10] is stated by the minimization of a functional J:

$$min \quad J(t, \mathbf{x}(t), \mathbf{u}(t)) = \mathbf{E}(t_f, \mathbf{x}(t_f)) + \int_{t_i}^{t_f} \mathbf{L}(\mathbf{x}(t), \mathbf{u}(t))dt.$$

subjected to: (OCP)

$\dot{x} = \mathbf{f}(\mathbf{x}(t), \mathbf{u}(t), \mathbf{p})$	dynamic equations;
$0 = \mathbf{g}(t, \mathbf{x}(t), \mathbf{u}(t), \mathbf{p})$	algebraic equations;
$\mathbf{x}(t_i) = \mathbf{x}_i$	initial boundary conditions;
$\psi(\mathbf{x}(t_f)) = 0$	final boundary conditions;
$\phi_\mathbf{l} \leq \phi[\mathbf{x}(t), \mathbf{u}(t), \mathbf{p}] \leq \phi_\mathbf{u}$	path constraints.

Where:

- Variable $t \in [t_i, t_f] \subset \mathbb{R}$ represents time.

Notice that the initial time t_i is fixed and the final time t_f might be fixed or left undetermined.

- $\mathbf{p} \in \mathbb{R}^{n_p}$ is a vector of parameters.
- $\mathbf{x}(t) : [t_i, t_f] \to \mathbb{R}^{n_x}$ represents the state variables.
- $\mathbf{u}(t) : [t_i, t_f] \to \mathbb{R}^{n_u}$ represents the control functions.
- J is he objective function : $[t_i, t_f] \times \mathbb{R}^{n_x} \times \mathbb{R}^{n_u} \times \mathbb{R}^{n_p} \to \mathbb{R}$.

It is given in Bolza form, expressed as the sum of the Mayer term $E(t_f, x(t_f))$ and the Lagrange term $\int_{t_i}^{t_f} L(x(t), u(t), p)dt$. Functions E : $[t_i, tf] \times \mathbb{R}^{n_x} \to \mathbb{R}$

and L : $\mathbb{R}^{n_x} \times \mathbb{R}^{n_u} \times \mathbb{R}^{n_p} \to \mathbb{R}$ are assumed to be twice differentiable.

The system is a Differential Algebraic Equations (DAE) system in which the right hand side function of the differential set of equations $\mathbf{f} : \mathbb{R}^{n_x} \times \mathbb{R}^{n_u} \times \mathbb{R}^{n_p} \to \mathbb{R}^{n_x}$ is assumed to be piecewise Lipschitz continuous, and the derivative of the algebraic right hand side function $\mathbf{g} : \mathbb{R}^{n_x} \times \mathbb{R}^{n_u} \times \mathbb{R}^{n_p} \to \mathbb{R}^{n_z}$ with respect to z is assumed to be regular.

- $\mathbf{x_i} \in \mathbb{R}^{n_x}$ represents the vector of initial conditions given at the initial time t_i.
- Function $\psi : \mathbb{R}^{n_x} \to \mathbb{R}^{n_q}$ provides the conditions at the final time.
- Function $\phi : \mathbb{R}^{n_x} \times \mathbb{R}^{n_u} \times \mathbb{R}^{n_p} \to \mathbb{R}^{n_\phi}$ represent the algebraic path constraints with lower bound $\phi_\mathbf{l} \in \mathbb{R}^{n_\phi}$ and upper bound $\phi_\mathbf{u} \in \mathbb{R}^{n_\phi}$.

Functions ψ and ϕ are assumed to be twice differentiable.

Applying this theory to the case of this study, the functional to optimize will be the fuel consumption that can be computed as the difference of the mass of the aircraft between the initial and final state: $Fuel\ burned = m(t_i) - m(t_f)$.

The dynamic system formed by the equations of motion of the aircraft must be properly defined depending on the type or dynamic mode: 3D, horizontal or vertical motion, constant rate of climb, etc.

Finally, boundary values and restrictions will arise from the particular characteristics of the model. They will depend on the specific flight plan (waypoints, departure procedures, etc.), aircraft flight envelope and others.

2.2 Multi-phase problem

The particularities of the problem lead the optimal control problem to be formulated with a multiphase approach. The multiphase optimal control problem must be conveniently formulated in order to get the optimization of the complete flight but with particular model elements for each phase.

Phases nature in flight optimization may have different inherent reasons like change in aerodynamic configuration of the aircraft, atmosphere model (troposphere or stratosphere), dynamic modes (as horizontal or vertical flight), etc. But they can be also introduced by the engineer to set particular

specifications like overflying a waypoint.

The formulation of the multi-phase problem involves the following elements:

- the performance index, typically rewritten as a sum of the individual performance indexes for each phase;
- differential equations and path constraints for each phase;
- phase linkage constraints which relate the states and time boundaries between phases;
- event constraints at initial and final states of some phases that must be satisfied.

The notation used to designate states, controls and variables of a phase is $\mathbf{x^{p_k}}$, $\mathbf{u^{p_k}}$ and $\mathbf{p^{p_k}}$ respectively, where k is the index denoting the number of the phase $k \in [1, \cdots, N_p]$. N_p is the number of phases.

As explained, the performance index for a multiphase flight will be sum of the performance indexes of the total number of phases:

$$J = \sum_{k=1}^{N_p} J^{p_k} \tag{2.1}$$

The objective to minimize along this report is the fuel. The performance index for a phase number n has been computed as the difference between the mass at the initial time of the first phase and the mass at the final time of the last one:

$$m_i^{p_{n_i}} - m_f^{p_{n_f}}$$

Note that $m_i^{p_n} > m_f^{p_n}$. The performance index for the minimum fuel consumption multiphase problem is the sum of the fuel consumed in each phase:

$$J = \sum_{k=1}^{N_p} (m_i^{p_k} - m_f^{p_k})$$

The linkage constraints are one of the key points in multiphase problems. These are applied to states and continuous variables linking the value at the final time of the previous phase and the value at the initial time of the current phase. The same way, the final value of the current phase must be equal to

the initial value of the following. They can be defined as equality constraints of the form:

$$x_f^{p_{n-1}} = x_i^{p_n} \tag{2.2a}$$

$$x_f^{p_n} = x_i^{p_{n+1}} \tag{2.2b}$$

In the case of waypoints, these are introduced between two phases and defined as equality restrictions as well. In fact, waypoints, is one of the causes of the multiphase definition of the flight optimization plan, since it forces to divide the problem in order to fix the restriction. A waypoint $(\theta_{WP}, \lambda_{WP})$ defined between phases n and n+1 would be denoted:

$$\lambda_f^{p_n} = \lambda_{WP}$$

$$\lambda_i^{p_{n+1}} = \lambda_{WP}$$

$$\theta_f^{p_n} = \theta_{WP}$$

$$\theta_i^{p_{n+1}} = \theta_{WP}$$

Waypoints are a type of event constraints, but also altitude or velocity restrictions can be set as equality constraints at initial or final states of a phase.

2.3 Solving methods

The numerical approaches to solve optimal control problems can be divided in three main families detailed in the points below.

- **Dynamic Programming (DP) methods [2]:** use the Hamilton-Jacobi-Bellman optimality criteria.
- **Indirect methods:** use calculus of variations and Pontryagin's Minimum Principle [9] to derive the necessary conditions of optimality. This conditions give as result a boundary value problem that arises from taking the derivative of a Hamiltonian. The boundary value problem is then discretize. Indirect methods require numerical root finding and ODE methods.
- **Direct methods:** discretize the continuous optimal control problem and construct a sequence of points. This gives a finite set of variables that can be solved using optimization methods. A typical strategy is to convert the problem into a nonlinear programming (NLP) problem which can be solved using mathematical programming techniques as

NLP methods. NLP techniques use Karush-Kuhn-Tucker (KKT) conditions to achieve local optimizations. Direct methods do not require explicit derivation and construction of the necessary conditions.

Dynamic programming divides the problem into subproblems that are linked together by a recurrence relation. The solution is found by recursive computations of the subproblems. The main drawback of the DP technique is its exponential increase of its size that makes it inadequate for large-scale problem as flight optimization, is the so-called "course of dimensionality". In addition, also problems arise from the nonsmoothless of the value function.

The indirect methods is a more tractable approach from the engineering point of view. It requires the formulation of the necessary conditions of optimality, for whose properly derivation is required a significant knowledge of optimal control theory. In addition, a simple modification of the model equations or constraints imply a reformulation of the adjoin equations. Furthermore, suitable initial guesses must be provided to start the iterative method and get a correct solution. The problem is that the adjoin equation usually do not have physical meaning and it may be difficult to solve even with physical reasonable initial guesses. This is because the Hamiltonian generates a boundary value problem with a great numerical sensitivity which may produce trajectories that exceed the numerical range of the computer.

While indirect methods follow a "first optimize, then discretize" approach, direct methods use the opposite: "first discretize, then optimize" technique. In this way, the infinite dimensional problem is converted into a finite dimensional one. Among the direct methods family, it can be differenced some different approaches. Direct single shooting methods allow an easy transformation of the optimal control problem to a Non-Linear Programming (NLP) problem. However, they are very sensitive to initial guess perturbations. Some of the problems are reduced with direct multiple shooting methods, but when including inequality restrictions, the constrained arcs must be specified in advance.

The best approach to solve aerospace trajectory optimization are direct collocation methods. Direct collocation methods include Hermite-Legendre-Gauss-Lobatto and pseudospectral approaches which apply local and global discretization of the set of equations formed by the DAE system, respectively. A deeper review of the theory on Pseudospectral methods can be found in next chapter for which it has been necessary the introduction of some of the common characteristics of the direct collocation methods family.

Chapter 3

Pseudospectral method

This section aims to review the theory of pseudospectral methods and detail the Legendre pseudospectral approach and its application to the flight optimization problem formulated as an optimal control problem. In order to develop this task it will be necessary the introduction of general concepts of the direct collocation methods family. With these methods it is possible to achieve an effective discretization of the DAE system formed by the dynamic equations of motion and the algebraic constraints and transform them into a set of algebraic equality constraints.

In order to apply the numerical approach given by direct collocation methods, the problem time interval is divided into segments by a definite grid of points covering the time interval $[t_i, t_f]$, $t_i = t_1 < t_2 \cdots < t_N = t_f$ and the decision variables (control and states) are characterized using interpolating polynomials at that grid points called collocation points. The main difference between Hermite-Simpson and pseudospectral method is that the first one uses local interpolating polynomials and the second parametrize the equations using global polynomials.

In a complete flight optimization problem, a large amount of variables and constraints can be involved obtaining very large NLP problems. However due to sparsity of the problem and the existence of efficient software, solution finding may be easier than for boundary-value problems.

Consider now the general optimal control problem defined in Section 2.1. By using direct collocation methods it is possible to discretize it to obtain a NLP problem of the form:

Chose $\mathbf{y} \in \mathcal{R}^{n_y}$ to minimize:

$$L(\mathbf{y})$$

subjected to:

$$\begin{bmatrix} \mathbf{0} \\ \mathbf{H_L} \\ \mathbf{\Psi_L} \end{bmatrix} \leq \begin{bmatrix} \mathbf{Z}(\mathbf{y}) \\ \mathbf{H}(\mathbf{y}) \\ \mathbf{\Psi}(\mathbf{y}) \end{bmatrix} \leq \begin{bmatrix} \mathbf{0} \\ \mathbf{H_U} \\ \mathbf{\Psi_U} \end{bmatrix} \tag{NLP}$$

$$\mathbf{y_L} \leq \mathbf{y} \leq \mathbf{y_U}$$

where:

- **L** is simply a mapping resulting from the evaluation of the performance index;
- **Z** is the mapping that arises from the discretization of the differential constraints over the grid points;
- **H** arises from the evaluation of the path constraints at each of the grid points, with associated bounds $\mathbf{H_L}$, $\mathbf{H_U}$;
- **Φ** is simply a mapping resulting from the evaluation of the event constraints.

3.1 Pseudospectral method theory

Pseudospectral methods use the combination of global orthogonal polynomial to approximate states and controls. A function is approximated as a sum of smooth functions which are often Legendre or Chebyshev polynomials. Collocation points depend on the interpolating polynomials used.

Theory shows that one of the main characteristics of pseudospectral methods is its exponential rate of convergence, faster than any other polynomial rate. This phenomena is widely illustrated in [12]. In addition, commonly, PS methods can achieve good accuracy with less collocation points. By contrast, the NLP associated to optimal problems approximated by pseudospectral methods use to be not as sparse as trapezoidal or Hermite-Simpson method which are derived from Runge-Kutta approaches. This results are usually more difficult to solve, slower and they may not work very well if solution is

not sufficiently smooth or the representation require many grid points.

Pseudospectral interpolating polynomials are typically defined over the interval $[-1, 1]$ so the optimal control problem must be mapped from $t \in [t_i, t_f]$ to $\tau \in [-1, 1]$ by using the transformation:

$$t = \frac{t_f + t_i}{2} + \frac{t_f - t_i}{2}\tau, \tag{3.1}$$

Each state and control variable is approximated using:

$$\mathbf{x}(\tau) \approx \tilde{\mathbf{x}}(\tau) = \sum_{k=0}^{N} \frac{W(\tau)}{W(\tau_k)} \mathbf{x}_k \phi_k(\tau); \tag{3.2a}$$

$$\mathbf{u}(\tau) \approx \tilde{\mathbf{u}}(\tau) = \sum_{k=0}^{N} \frac{W(\tau)}{W(\tau_k)} \mathbf{u}_k \phi_k(\tau); \tag{3.2b}$$

where k is the index of the nodes of the interpolating polynomial of order N ($k = (0, \ldots, N)$), $W(\tau)$ denotes a positive weight function, x_k and y_k are values of the states and controls for node k, and $\phi_k(\tau)$ is the general expression fora a Lagange interpolating polynomial of degree N that satisfies:

$$\phi_k(\tau) = \prod_{i=0, i\neq k}^{N} \frac{\tau - \tau_i}{\tau_k - \tau_i}. \tag{3.3}$$

Where i denotes another index indicating the node for the global Legendre interpolating polynomial. It should be noted that $\phi_k(\tau_i) = 1$ if $k = i$ and $\phi_k(\tau) = 0$ if $k \neq i$.

The first derivative of each of the states and controls 3.2 is given by the following equations:

$$\dot{\mathbf{x}}(\tau_j) \approx \dot{\tilde{\mathbf{x}}}(\tau_j) = \sum_{k=0}^{N} \mathbf{x}_k \dot{\phi}_k(\tau_j) = \sum_{k=0}^{N} D_{jk} \mathbf{x}_k; \tag{3.4a}$$

$$\dot{\mathbf{u}}(\tau_j) \approx \dot{\tilde{\mathbf{u}}}(\tau_j) = \sum_{k=0}^{N} \mathbf{u}_k \dot{\phi}_k(\tau_j) = \sum_{k=0}^{N} D_{jk} \mathbf{u}_k. \tag{3.4b}$$

3.1.1 Legendre pseudospectral method

Legendre functions L_k, $k = 0, 1, \ldots, N$, are the solutions to the Legendre differential equations defined by:

$$\frac{d}{d\tau}\left[(1-\tau^2)\frac{d}{d\tau}L_k(\tau)\right] + k(k+1)L_k(\tau) = 0; \tag{3.5}$$

whose solution satisfies the following relation:

$$L_{k+1}(\tau) = \frac{2k+1}{k+1}\tau L_k(\tau) - \frac{k}{k+1}L_{k-1}(\tau). \tag{3.6}$$

The Legendre pseudospectral method is based on interpolating functions on Legendre-Gauss-Lobatto (LGL) collocation points.

The choice of the collocation points type is carried out depending on the kind of interpolating polynomial and is an important factor for success in the solution. In case of finite horizon problems with any either fixed or free boundary conditions, the Legendre-Gauss-Lobatto (LGL) collocation points are chosen.

LGL collocation points include points at $\tau_0 = -1$ and $\tau_N = 1$. Intermediate points τ_k where $k = (1, \ldots, N-1)$ are the roots obtained from $\dot{L}_N(\tau)$. In addition weight functions in Equations 3.2 is $W(\tau) = 1$.

In the case of LGL collocation points, the Lagrange interpolating polynomial of order N is given by:

$$\phi_k(\tau) = \frac{1}{N(N+1)L_N(\tau_k)}\frac{(\tau^2-1)\dot{L}_N(\tau)}{\tau - \tau_k}, \tag{3.7}$$

and the derivation matrix yields:

$$D_{jk} = \begin{cases} \frac{L_N(\tau_j)}{L_N(\tau_k)}\frac{1}{\tau_j - \tau_k} & \text{for } j \neq k \\ -\frac{(N+1)N}{4} & \text{for } j = k = 0 \\ \frac{(N+1)N}{4} & \text{for } j = k = N \\ 0 & \text{otherwise.} \end{cases} \tag{3.8}$$

Example of a Legendre pseudospectral method application

In order to introduce the Legendre application, a simple differentiation of a function has been studied.

Figure 3.1 shows Legendre differentiation of function

$$f(\tau) = \frac{sin(3\tau)}{e^{\tau}}$$

for different number of nodes (N = 5, 10, 15 and 20) using Legendre pseudospectral approach.

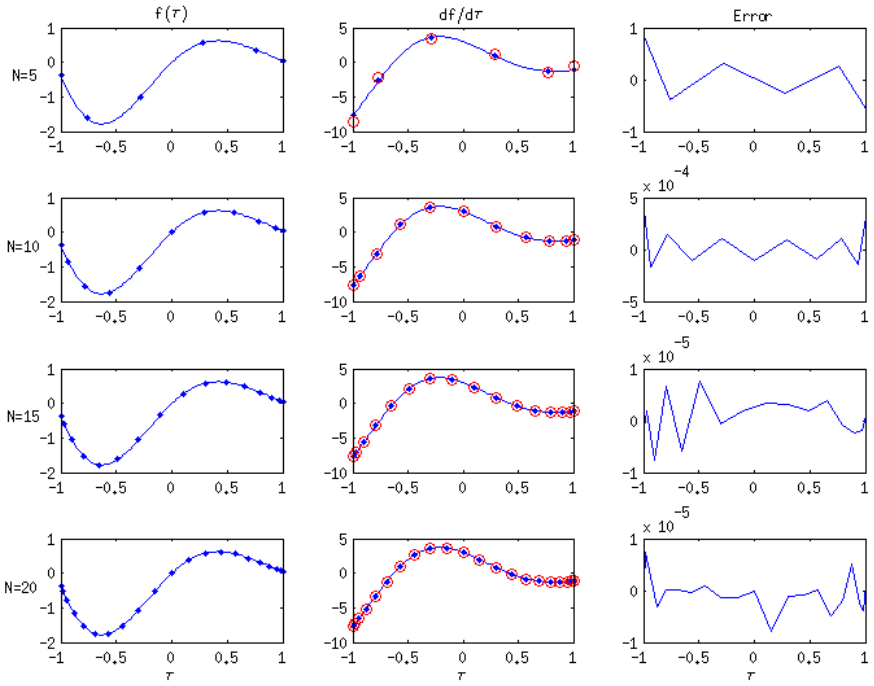

Figure 3.1: *Legendre differentiation of function* $f(\tau)$

First column shows the discretization of the collocation points, τ_k, over the function $f(\tau)$. Second column shows the results obtained with Legendre method for the derivative of $f(\tau)$ with respect to τ. It has been computed using Equation 3.4 after computing derivative matrix D for the different values of N.

These results have been displayed with small red circles over the analytical solution given by function: $df/d\tau = (3\cos(3\tau)e^{\tau} - \sin(3\tau)e^{\tau})/e^{2\tau}$.

Finally, the error has been computed and displayed in the last column just by subtracting the numerical solution from the analytical one.

It must be noticed the orders of magnitude of the errors for the different vales of N that decrease for increasing number of nodes.

3.2 Solving the optimal control problem with Legendre pseudospectral method

Consider now the general control problem shown in Section 2.1. As it was explained, the problem consist of finding the states, $\mathbf{x}$, and controls, $\mathbf{u}$, to minimize a performance index in a finite time t. Applying pseudospectral necessary time mapping, $t \in [t_i, t_f]$ is transformed into $\tau \in [-1, 1]$.

The problem is subjected to a set of equations of motion which are described by first order ODEs. These dynamic equations must be rewritten to the form:

$$\dot{\mathbf{x}}(\tau) = \frac{t_f - t_i}{2} \cdot \mathbf{f}(\mathbf{x}(\tau), \mathbf{u}(\tau), p). \tag{3.9}$$

Also path constraints and algebraic equations must be rewritten to:

$$\phi(\tau)[\mathbf{x}(\tau), \mathbf{u}(\tau), p] \leq \mathbf{0}; \tag{3.10}$$

$$\mathbf{0} = \mathbf{g}[\mathbf{x}(\tau), \mathbf{u}(\tau), p]. \tag{3.11}$$

Applying Legendre pseudospectral approximation to states and controls, $\tilde{\mathbf{x}}(\tau)$ and $\tilde{\mathbf{u}}(\tau)$ are approximated using Equations 3.2. Note that in the case of the optimal control problem we are dealing with, $\tilde{\mathbf{x}}(\tau) = \mathbf{x}(\tau)$ and $\tilde{\mathbf{u}}(\tau) = \mathbf{u}(\tau)$.

The derivative of the state vector $\dot{\tilde{\mathbf{x}}}(\tau_j)$ is approximated using 3.4, where D is computed as a function of the number of nodes, N, of the phase.

Consider now the following matrices:

- Matrix $\mathbf{U}$ with dimensions $x_u \times (N+1)$ stores the trajectories of the controls at LGL nodes:

$$\mathbf{U} = [\mathbf{u}(\tau_0), \mathbf{u}(\tau_1), \cdots, \mathbf{u}(\tau_N)]. \tag{3.12}$$

- Matrices $\mathbf{X}$ and $\dot{\mathbf{X}}$ with dimensions $x_x \times (N+1)$ stores the trajectories of the states and their approximate derivatives at LGL nodes:

$$\mathbf{X} = [\mathbf{x}(\tau_0), \mathbf{x}(\tau_1), \cdots, \mathbf{x}(\tau_N)]; \tag{3.13}$$

$$\dot{\mathbf{X}} = [\dot{\tilde{\mathbf{x}}}(\tau_0), \dot{\tilde{\mathbf{x}}}(\tau_1), \cdots, \dot{\tilde{\mathbf{x}}}(\tau_N)]. \tag{3.14}$$

- Matrix $\mathbf{F}$ with dimensions $x_x \times (N+1)$ contains the right hand side of differential constraints evaluated at LGL nodes:

$$\mathbf{F} = \frac{t_f - t_i}{2} \left[\mathbf{f}[\mathbf{x}(\tau_0), \mathbf{u}(\tau_0), \mathbf{p}, \tau_0], \cdots, \mathbf{f}[\mathbf{x}(\tau_N), \mathbf{u}(\tau_N), \mathbf{p}, \tau_N]\right]. \tag{3.15}$$

Then, the differential equations are transformed into algebraic constraints expressed as:

$$[\dot{\mathbf{X}} - \mathbf{F}] = [\mathbf{X}\mathbf{D}^{\mathbf{T}} - \mathbf{F}] = 0 \tag{3.16}$$

and the decision vector $\mathbf{y}$ as:

$$\mathbf{y} = \begin{bmatrix} \mathbf{U} \\ \mathbf{X} \\ \mathbf{p} \\ t_i \\ t_f \end{bmatrix}. \tag{3.17}$$

The problem to solve is the NLP problem described in the introduction of this chapter.

As explained in Section 1.3, for the development and resolution of the flight optimization problem developed in this study, AMPL programming language has been used together with IPOPT nonlinear solver.

Chapter 4

Models

In this chapter, the model used to represent the flight model is presented. Despite of the fact that the whole model must be coherent together, it has been divided in different sections in order to make it easier to understand. The model has a continuous part since the states included in the equations of motion (x, y, h, V, γ, μ, χ, and m) follow a continuous distribution along the flight. Earth and atmospheric parameters depend mainly on the altitude and follow continuous distributions as well. By contrast, controls and related parameters can follow non-continuous distributions along the trajectory. These states and controls can be subjected to different constraints, dynamic modes, limitations, etc. which leads to a division of the flight in phases. In other words, the flight of an aircraft has a multi-stage nature due to:

- different aircraft Aerodynamic Configurations (AC),
- Dynamic Modes (DM),
- Atmosphere Modes (AM),
- Operative Procedures (OP),
- wayoints (WP).

For the derivation of the model, some general hypothesis have been applied leading to the following assumptions:

- Flat and non-rotating Earth model.
- Earth inertial reference frame $F_e(O_e, x_e, y_e, z_e)$.

- Point mass model: transnational equations are uncoupled from rotational equations. All forces apply on the centre of gravity of the aircraft.
- Parabolic drag polar.
- Fixed engines and small thrust angle of attack.
- Standard atmosphere model: ISA.
- Moving atmosphere: wind is considered.

4.1 Flight model

4.1.1 3D equations of motion

Applying the assumptions corresponding to the aircraft performance, the motion of the aircraft can be modelled with the 3-DOF equations of motion defined by the following set of Ordinary Differential Equations (ODE):

$$\dot{x} = V\cos(\gamma)\cos(\chi) + w_x \tag{4.1a}$$

$$\dot{y} = V\cos(\gamma)\sin(\chi) + w_y \tag{4.1b}$$

$$\dot{h} = V\sin(\gamma) \tag{4.1c}$$

$$\dot{V} = \frac{Thr - D - mg\sin(\gamma)}{m} \tag{4.1d}$$

$$\dot{\chi} = \frac{L\sin(\mu)}{mV\cos(\gamma)} \tag{4.1e}$$

$$\dot{\gamma} = \frac{L\cos(\mu) - mg\cos(\gamma)}{mV} \tag{4.1f}$$

$$\dot{m} = -Thr \cdot \eta \tag{4.1g}$$

where:

- x and y h are the down range (or longitude), cross range (or latitude) and altitude parameters that give the position of the aircraft
- V is the true air airspeed (TAS) of the aircraft
- w_x and w_y are the wind velocities in x and y direction

- m is the mass
- g is the acceleration due to gravity
- L and D are the lift and drag forces
- Thr is the thrust or propulsive force generated by the engines
- γ, χ and μ are the flight-path, heading and bank angles respectively

4.1.2 Dynamic modes

Dynamic modes arise from the restriction of the motion to lay in a certain plane. Due to flight requirements, in the case of study, several phases apply a vertical or horizontal motion restriction. Before that, horizontal an vertical motion phases have been implemented in the introductory problems (Chapter 5). The first introductory problem (Section 5.1) shows a single phase with motion in an horizontal plane. In the second introductory problem (shown in Section 5.2), a 2D complete flight (vertical motion) optimization problem is solved.

Vertical motion (VM)

The motion of the aircraft is constrained to a vertical plane. This leads to a constant course, i.e., constant heading angle χ.

$$\chi = const.$$

Assuming a levered flight it can be proof that the bank angle is zero:

$$\mu = 0$$

In a 3D vertical flight where position is determined by latitude, longitude and height (or x, y, h), then, Equation of Motion 4.1e does not apply:

$$\dot{x} = V\cos(\gamma)\cos(\chi) + w_x \tag{4.2a}$$

$$\dot{y} = V\cos(\gamma)\sin(\chi) + w_y \tag{4.2b}$$

$$\dot{h} = V\sin(\gamma) \tag{4.2c}$$

$$\dot{V} = \frac{Thr - D - mg\sin(\gamma)}{m} \tag{4.2d}$$

$$\dot{\gamma} = \frac{L - mg\cos(\gamma)}{mV} \tag{4.2e}$$

$$\dot{m} = -Thr \cdot \eta \tag{4.2f}$$

In case of a 2D flight where the position of the aircraft is contained in a plane longitude-altitude (x,h), heading angle is zero:

$$\chi = 0$$

In addition, lateral forces and wind can be neglected and equations of motion can be reduced to:

$$\dot{x} = V\cos(\gamma) + w_x \tag{4.3a}$$

$$\dot{h} = V\sin(\gamma) \tag{4.3b}$$

$$\dot{V} = \frac{Thr - D - mg\sin(\gamma)}{m} \tag{4.3c}$$

$$\dot{\gamma} = \frac{L\cos(\mu) - mg\cos(\gamma)}{mV} \tag{4.3d}$$

$$\dot{m} = -Thr \cdot \eta \tag{4.3e}$$

Horizontal motion (HM)

In an horizontal flight, the motion is constrained to a constant altitude:

$$h = const.$$

Since the aircraft has not the possibility to pitch up or down:

$$\gamma = 0$$

If the phase belongs to a 3D problem, the motion is constrained to a latitude-longitude (or x-y) plane, turning out into a 2D phase modeled with equations of motion:

$$\dot{x} = V\cos(\gamma)\cos(\chi) + w_x \tag{4.4a}$$

$$\dot{y} = V\cos(\gamma)\sin(\chi) + w_y \tag{4.4b}$$

$$\dot{V} = \frac{Thr - D}{m} \tag{4.4c}$$

$$\dot{\chi} = \frac{L\sin(\mu)}{mV} \tag{4.4d}$$

$$\dot{m} = -Thr \cdot \eta \tag{4.4e}$$

In case of a 2D flight problem an horizontal motion phase would get reduced to a 1D flight governed by equations:

$$\dot{x} = V\cos(\gamma) + w_x \tag{4.5a}$$

$$\dot{V} = \frac{Thr - D}{m} \tag{4.5b}$$

$$\dot{m} = -Thr \cdot \eta \tag{4.5c}$$

4.1.3 Operative procedures and constraints

Air navigation restrictions include operative procedures in departure and approaching, overflying waypoints, altitude, thrust and velocity constraints, ect.

These kind of restrictions force the problem to be divided into different phases and to introduce equality constraints at the initial and final states of them as explained in Section 2.2

4.2 Earth model

The Earth is considered flat, non rotating, and approximate inertial reference frame. Since, locations in Earth are given in spherical coordinates expressed as latitude (θ) and longitude (λ) positions, the following approximation has been carried out:

$$x = \lambda \cdot r \cdot \cos(\theta) \tag{4.6a}$$

$$y = \theta \cdot r \tag{4.6b}$$

where r is the distance to the centre of the Earth, i.e., $r = R_{Earth} + h$.

Regarding the gravitational acceleration, it has been applied an altitude correction $g = m_{Earth} \cdot G_{grav}/r^2$, where $m_{Earth} = 5.9736^{24}[Kg]$ is the mass of the Earth and $G_{grav} = 6.6742^{-11}[N \cdot m^2/kg^2]$ is the universal gravitational constant.

4.3 Atmosphere model

The atmosphere variables have been computed applying the well-known ISA Atmosphere model. The temperature gradient in the troposphere is constant ($\beta_T = -0.0065\ [K/m]$) and in the inferior part of the stratosphere the temperature is constant. The perfect gas equation applies in the model.

- **Troposphere** ($0 \leq h \leq 11000[m]$)

$$T = T_0 + \beta_T \cdot h[m] \tag{4.7}$$

- **Inferior part of the Stratosphere** ($11000[m] \leq h[m] \leq 20000[m]$)

$$T = T_{trop} = T_0 + \beta_T \cdot 11000 \tag{4.8}$$

The density, pressure, and sound velocity are then computed as:

$$\frac{\rho}{\rho_{0_{ISA}}} = \left(1 + \frac{T_{0_{ISA}} + \beta_T \cdot h[m]}{T_{0_{ISA}}}\right)^{\frac{-g}{R_{air} \cdot \beta_T}} \tag{4.9}$$

$$\frac{p}{p_{0_{ISA}}} = \left(\frac{T_{0_{ISA}} + \beta_T \cdot h[m]}{T_{0_{ISA}}}\right)^{\frac{-g}{R_{air} \cdot \beta_T}} \tag{4.10}$$

$$a = \sqrt{\gamma_{air} R_{air} T} \tag{4.11}$$

where $\gamma_{air} = 1.4$, $R_{air} = 287.052[J/(Kg \cdot K)]$ and:

- $T_{0_{ISA}} = 288.15\ [K]$ is the standard atmospheric temperature at Mean Sea Level (MSL);
- $p_{0_{ISA}} = 101325\ [Pa]$ is the standard atmospheric pressure at MSL;
- $\rho_{0_{ISA}} = 1.225\ [kg/m^3]$ is the standard atmospheric density at MSL.

T_0 is computed as $T_{0_{ISA}} + \Delta T$, where $\Delta T > 0$ for hot days and $\Delta T < 0$ for cold days. Through the whole development of the problem, it has been considered $\Delta T = 0$, hence $T_0 = T_{0_{ISA}}$.

4.3.1 Wind model

The model developed to represent the wind conditions and explained below has been taken from [11]. The raw data given by the forecast is a set of values of the wind in x (longitude λ) direction and y (latitude, θ) direction for a grid of positions (λ, θ) on the earth surface. These data has been converted into analytic functions by mean of a nonlinear regression valid within a domain.

Application of the wind model is introduced in the third introductory problem shown in Section 5.3. In the case study, wind model has been only applied in phases 9 to 14 (both of them included). It must be noticed that, for sake of simplicity, wind model considers the same wind condition regardless of the altitude since wind is only affecting cruise phases where height changes in an small range.

4.4 Aircraft Model

The aircraft chosen has been the Airbus-A320 modelled following the BADA specifications [6]. Aircraft BADA model defines the different parameters relative to mass, aerodynamic configurations (AC), performance limitations (flight envelope), engine thrust, fuel flow, etc. In Annex I, these parameters are collected.

In general, five aerodynamic configurations can be distinguished: take off (TO), initial climb (IC), cruise (CR), approach (AP) and landing (LD).

4.4.1 Aerodynamics

The aircraft is considered to fly in a incompressible subsonic regime so that the effects of Mach number can be neglected. In addition the model does not take into account lateral aerodynamic forces assuming them sufficiently small. This leads in that the two main aerodynamic forces are lift (L) and drag (D). The dimensional forces can be computed as:

$$C_L = \frac{L}{\frac{1}{2}\rho V^2 S}; \tag{4.12a}$$

$$C_D = \frac{D}{\frac{1}{2}\rho V^2 S}. \tag{4.12b}$$

In general C_L can be modelled as a linear function of the angle of attack, α, and in the case of study is a free control system, except from horizontal motion in which lift must equal the product $m \cdot g$. Drag coefficient is related to lift coefficient following the parabolic drag polar expressed as:

$$C_D = C_{D_{0,AC}} + C_{D_{i,AC}} \cdot C_L^2 \tag{4.13}$$

where C_{D_0} is the parasite drag coefficient and C_{D_i} is the induced coefficient. Note that BADA model provides both C_{D_0} and C_{D_i} for the five different aircraft configurations (AC stands either for TO, IC, CR, AP or LD). In addition during landing phase, the drag increase produced by the landing gear is taken into account by adding the coefficient $C_{D_{0,\Delta LD}}$:

$$C_D = C_{D_{0,LD}} + C_{D_{0,\Delta LD}} + C_{D_{i,LD}} \cdot C_L^2. \tag{4.14}$$

4.4.2 Flight envelope

For aerodynamic and structural reasons, velocity in terms of true airspeed (V), calibrated airspeed (V_{CAS}) or Mach ($M = V/a$) is limited following the restrictions detailed below.

The velocity is limited to the maximum operating speed (CAS): V_{MO}:

$$V_{CAS} < V_{MO} \tag{4.15}$$

and the V_{CAS} is computed as:

$$V_{CAS} = \sqrt{\frac{2P_0}{\mu\rho_0}\left[\left(1 + \frac{P}{P_0}\left(1 + \frac{\mu\rho}{2P}V^2\right)^{\frac{1}{\mu}} - 1\right)^{\mu} - 1\right]} \tag{4.16}$$

where $\mu = (\gamma_{air} - 1)/\gamma_{air}$.

The Mach number can not exceed the maximum operational Mach number: M_{MO}:

$$M < M_{MO}. \tag{4.17}$$

In addition during flight, in order to avoid stall, velocity must be grater that V_{min} which is computed as the stall velocity $V_{stall,AC}$ times a safety coefficient:

$$V < V_{min} \tag{4.18}$$

with:

$$V_{min} = C_{V_{min}} \cdot V_{stall,AC}. \tag{4.19}$$

Note again that aerodynamic configuration is considered. $C_{V_{min}}$ is 1.3 for TO and 1.2 for the rest of configurations.

The maximum permitted altitude is computed as the minimum of the maximum operating altitude above standard MSL: h_{MO} and the maximum altitude above standard MSL at MTOW under ISA conditions, h_{max}, corrected for mass:

$$h_{max/act} < h_{MO} \tag{4.20}$$

$$h_{max/act} < h_{max} + G_w(m_{max} - m) \tag{4.21}$$

where G_w is the corrective mass gradient.

BADA model includes in the h_{max} correction the effect of temperature deviation from ISA conditions, but as explained in Section 4.3, ΔT has been considered null.

4.4.3 Engine thrust

In the optimization problem, thrust is a control limited in the BADA model by the maximum thrust Thr_{max}:

$$Thr < Thr_{max} \tag{4.22}$$

where:

$$Thr_{max} = C_{T_{c1}}(1 - \frac{h}{C_{T_{c2}}} + C_{T_{c3}}h^2) \cdot (1 + C_{T_{c5}}C_{T_{c4}}). \tag{4.23}$$

Equation 4.23 is valid only for jets. Note that it is function of the altitude.

Thrust can be described as a function of the maximum thrust by mean of throttle control pi:

$$Thr = \pi \cdot Thr_{max} \tag{4.24}$$

with $\pi \in [0, 1]$.

4.4.4 Fuel consumption

In concordance with Equation of Motion 4.1g, the fuel flow is defined as $\dot{m} = -Thr \cdot \eta$. BADA model for thrust specific fuel consumption $\eta[Kg/(min \cdot kN)]$ is computed for jets as:

$$\eta = C_{f1}\left(1 + \frac{V}{C_{f2}}\right). \tag{4.25}$$

In cruise configuration, η must be multiplied by C_{fcr}.

Fuel flow cannot descend, either in thrust or descend conditions, below $\dot{m}_{min}$ which is defined as:

$$\dot{m}_{min} = C_{f3}\left(1 - \frac{h}{C_{f4}}\right). \tag{4.26}$$

C_{f1}, C_{f2}, C_{f3},C_{f4} and C_{fcr} are operation performance parameters described in BADA model.

4.4.5 Operative restrictions

In addition to the restrictions presented along the model review, some more are included.

The model considers maximum values for acceleration for civil flights in longitudinal direction ($a_{l_{max}}$) and normal direction ($a_{n_{max}}$):

$$a_{l_{max}} = 2[ft/s^2]; \tag{4.27a}$$

$$a_{n_{max}} = 5[ft/s^2]. \tag{4.27b}$$

Also restrictions are applied to the bank angle whose maximum values for TO, and the rest of configurations is:

$$\phi_{max_{TO}} = \pm 25^0; \tag{4.28a}$$

$$\phi_{max} = \pm 45^0. \tag{4.28b}$$

Chapter 5

Introductory problems

This section aims to introduce the different key points of the complete flight optimization by mean of three introductory problems. This lets the discussion of some results that afterwards will help to understand the case study solution.

- The first problem deals with a 1D cruise with required time of arrival (RTA) solved for one and two phases. This way, it will be introduced a solution for a simple multiphase problem.
- The second introductory problem aims to obtain a full 2D flight, which is a well-known solution in flight optimization. In this case it has been divided the problem in 5 phases including different aerodynamic conditions, under and over tropopause atmosphere, etc.
- In the third case, a 3D model has been used to simulate a climb and the effect of the wind has been included.

5.1 Unidimensional cruise with required time of arrival

This introductory problem has been the starting point of the implementation of this study. The solution to this problem is presented in paper [8], which includes the results obtained using different collocation methods and an interesting comparative analysis is carried out. The scope of this report is out of the comparison among collocation methods. Instead, the problem has been solved using only Legendre pseudospectral methods and modelling the problem with a one-phase and two-phases approach.

The problem focuses on finding the optimal fuel consumption for a A320 aircraft in a unidimensional cruise phase. The model used is represented by Equations of Motion 4.5, i.e. 1D horizontal motion. It has been considered a flight from longitude $x_i = 0$ to $x_f = 1000\ km$ at constant altitude $h = 10000\ m$. The required time of arrival (RTA) is $t_f = 4751\ s$. The aircraft aerodynamic configuration is cruise (CR).

The boundary conditions are collected in Table 5.1. The parameters fixed, in addition to those already defined, are the initial mass (m_i) and the initial velocity (v_i). Note that the final velocity and mass are free.

Time t[s]	0	4751
Longitude x[km]	0	1000
Velocity v[kts]	420	Free
Mass m[kg]	51200	Free

Table 5.1: *Boundary conditions of 1D cruise with RTA*

The results presented in Figures 5.2 and 5.1 correspond to the numerical discretization using Legendre-Gauss-Lobatto technique. Results plotted in blue are the corresponding to one-phase model and the red one to 2-phases model. In addition the change of phase has been indicated at $t_{1,2}$ with a dashed grey line for the second case. The solution shown correspond to 30 nodes discretization in the case of the 1-phase model and 15 nodes in each phase of the 2-phases solution.

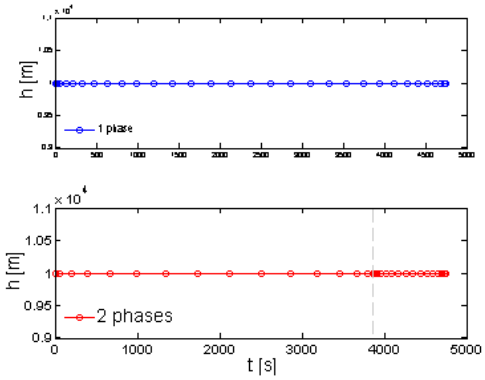

Figure 5.1: *Altitude profile of 1D cruise with RTA introductory problem*

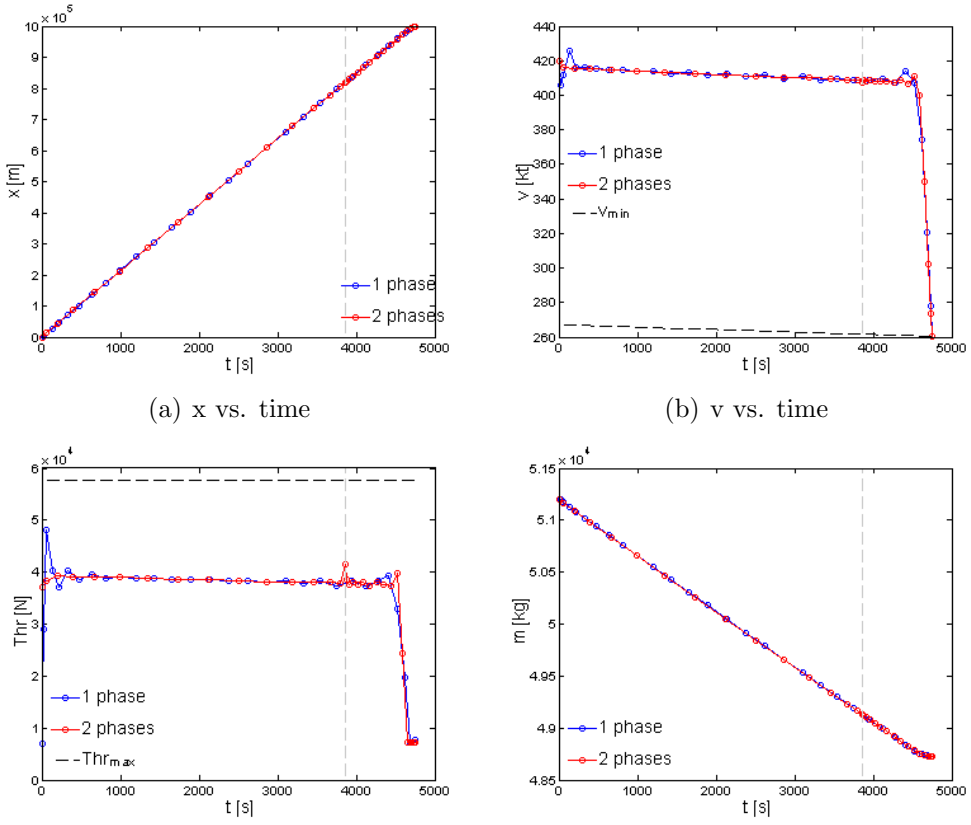

(a) x vs. time

(b) v vs. time

(c) Thr vs. time

(d) m vs. time

Figure 5.2: *States and controls of 1D cruise with RTA introductory problem*

In the one-phase model, the 1D motion is defined for the hole trajectory by meand of three equations of motion. In the case of the two-phases approach, the same equations of motion than in the one-phase model has been used for both phases.

Since the altitude is constant and the wind is not taken into account, the atmosphere model is reduced to constant parameters in terms of temperature, density, velocity of sound, etc. In both cases, the inequality constraints applied are the included in Section 4.4 for velocity (v, v_{CAS}, M), lift coefficient (C_L), fuel flow ($\dot{m}$) and acceleration ($\dot{v}$). In the 2-phases problem, these inequality constraints have been duplicated to apply in both phases.

In addition, equality constraints has been applied for initial and final states

points to set the boundary conditions. In the case of 2-phases problem, the initial boundary values has been applied on the initial disccretization points of the first phase states, and the final boundary conditions to the final grid points of second phase. Furthermore, one of the key-points of multiphase problem is the linkage between state variables of both phases. This joint task has been defined as:

$$\mathbf{x}_f^{p_1} = \mathbf{x}_i^{p_2}$$

applying multiphase approach explained in Section 2.2.

Below it is shown the minimum consumption obtained for both approaches:

1-phase model	Fuel consumption = 2472.63 kg
2 phases model	Fuel consumption = 2472.33 kg

The difference is very small and is only caused by approximating reasons. Figure 5.1 is a trivial solution, but the reason why it has been plotted is to see the nodes distribution and the change of phase at $t^{p_{1,2}} = 3863$ s. The change of phase at such time is because the solver finds the optimal solution at that conditions because of geometrical reasons due to polynomial approximation. It has been proved that for different distributions of nodes always adding up 30 total nodes, the change of phase instant changes considerably without changing the consumption value. In fact, this value could be any of the range of time without affecting appreciably the result.

Since the problem fixes the time of arrival, the solution focuses on finding the states and controls optimum distribution. The solution shows a slightly decreasing velocity up to the part of the time range in which decreases up to stall. Thrust decreases also to achieve this condition which is not a realistic result but is the optimality condition for this problem.

Thrust is the only control involved in this problem since lift must equal $m \cdot g$. Its plot, Figure 5.2(c), shows the numerical deviation at initial, final and interphase points which is a common result obtained in certain variables due to approximation reasons. The longitude increases almost linearly (slightly decreasing velocity) except from the last part in which the motion decelerates. Mass decreases linearly up to the final moments in which the already mentioned result saves some fuel.

5.2 2D complete flight optimization

This second introductory problem aims to solve another typical flight optimization problem: 2D flight. In this particular case, the problem objective is to find the minimum fuel consumption for a flight of 1000 km length with departure and arrival altitude $h_i = h_f = 0\ m$. The problem could have been solved using only one phase with the same aerodynamic configuration and atmosphere model along the trayectory. Despite, in order to make it more realistic and to introduce new concepts, it has been considered 5 phases.

Phase	Nodes	Atmosphere mode	Aerodynamic mode
1	10	*Below*	*IC*
2	14	*Below*	*CR*
3	30	*Above*	*CR*
4	18	*Below*	*CR*
5	8	*Below*	*AP*

Table 5.2: *Phase details of 2D flight introductory problem*

Table 5.2 shows the information corresponding to each phase. The flight includes initial climb (IC) and final approach)AP) phases. The IC phase has been fixed to finish at altitude $h^{p_{1,2}} = 13000\ ft$ ($\approx 3962.4\ m$) and the AP phase to start at $h^{p_{1,2}} = 6000\ ft$ ($\approx 1828.8\ m$). In addition, during the cruise aerodynamic mode phase, an intermediate division of the problem has been necessary in order to include above-tropopause conditions. The number of nodes in each phase has been distributed as a function of the expected length.

The data corresponding to boundary conditions and interphase constraints is collected in Table 5.3:

State	**Intial**	**1-2**	**2-3**	**3-4**	**4-5**	**Final**
Time t [s]	0	*Free*	*Free*	*Free*	*Free*	*Free*
Altitude h [ft]	0	13000	36000	36000	2000	6000
Longitude x [km]	0	*Free*	*Free*	*Free*	*Free*	1000
Velocity v [kt]	120	*Free*	*Free*	*Free*	*Free*	*Free*
Flight path angle γ [kg]	*Free*	*Free*	*Free*	*Free*	*Free*	*Free*
Mass m [kg]	64000	*Free*	*Free*	*Free*	*Free*	*Free*

Table 5.3: *Boundary conditions of 2D flight introductory problem*

The characteristic altitude profile obtained is shown in Figure 5.3. In this figure and the following, dashed grey lines have been displayed at the time at which the change of phases are produced. Furthermore, at tropopause altitude, i.e. approximately 36000 ft ($\approx$ 11000 m) height, a blue dotted line has been plotted. It can be seen how a greater number of nodes concentrates near interphase points due to LGL grid points distribution.

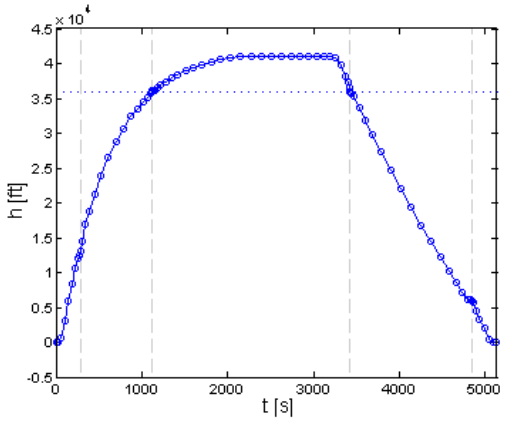

Figure 5.3: *Altitude profile of 2D flight introductory problem*

Equations governing the motion of the 5 phases correspond to a 2D vertical motion contained in the $x - h$ plane (Eq. 4.3). Results obtained for states (x,v,γ and m) and controls (Thr and C_L) are collected in Figure 5.4.

From the physical point of view, the optimum solution follows a flight with three well-differentiated phases in terms of performance (leaving aside the phases in which the problem was formulated): initial climb, cruise and approach. The initial climb is developed with a progressive change in the flight path angle up to cruise trajectory at constant altitude. The initial climb is carried out at maximum thrust reachable which is inversely proportional to the altitude. The velocity during this phase increases up to the maximum velocity reached. The cruise altitude is one of the main optimal results because it is given at maximum altitude defined by flight envelope restrictions (Section 4.4.2). This result is due to a lower density and favourable conditions in terms of drag force for higher altitudes. The cruise conditions match with a constant velocity and throttle and slightly decreasing lift coefficient.

At certain time, the aircraft starts descending suddenly. At this point, the thrust turns to the minimum possible value given by minimum fuel flow conditions, which is also an inverse function of the altitude.

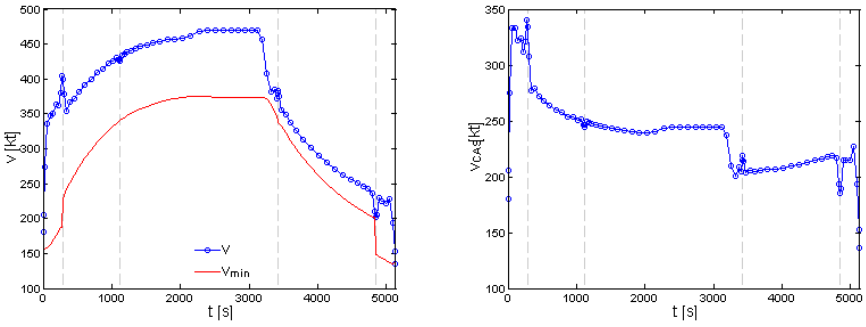

(a) v vs. time

(b) v_{CAS} vs. time

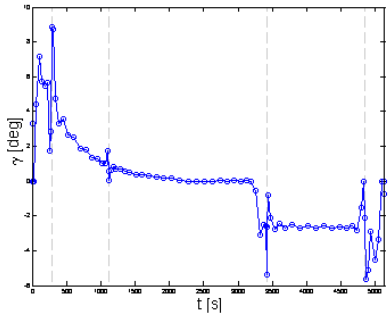

(c) γ vs. time

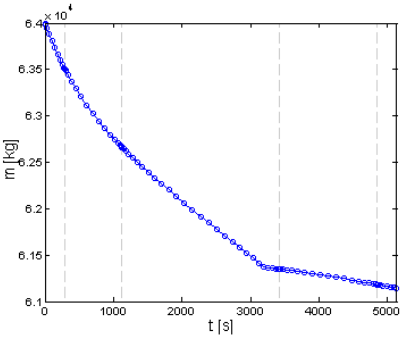

(d) m vs. time

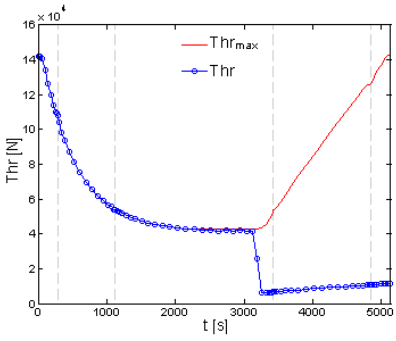

(e) Thr vs. time

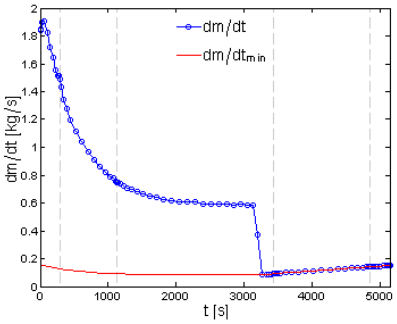

(f) $\dot{m}$ vs. time

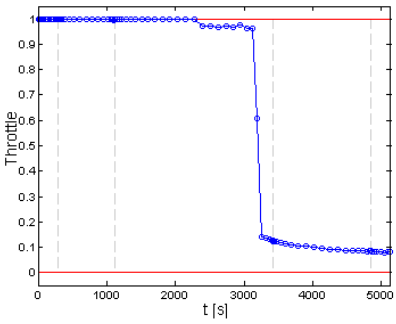

(g) Throttle vs. time

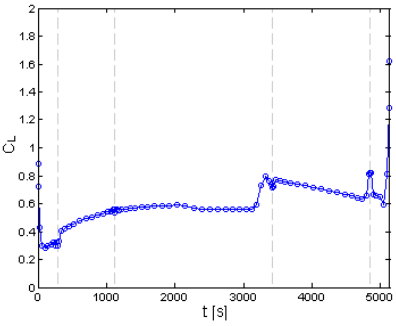

(h) C_L vs. time

Figure 5.4: *States and controls of 2D flight introductory problem*

Due to these well-differentiated phases in terms of thrust use, the mass experiments a faster waste of fuel up to that point and a slower consume in the last part of the flight to give the optimal result. Another important aspect, is the fact that, as in the previous problem, the solution tries to save fuel stalling the velocity at the final point. Regarding lift coefficient control, during climbing the lift coefficient increases up to cruise conditions are reached. As already said, during constant altitude and velocity cruise, the lift coefficient decreases due to decrease of mass. Finally during approach, C_L increases to hold smaller velocities.

Regarding now the solution from the mathematical point of view, it must be noticed that the solution has some deviations in the initial and final points of the phases given by polynomial approximation. These deviations arise in a more visible manner in flight path angle γ plot and is due to the difference in the order of magnitude with the rest of the states. γ takes values between $\pm 0.1745\ rad$ ($\approx \pm 10^0$) while other values as the longitude x can reach values of order of magnitude of $10^6\ m$.

5.3 3D cruise under wind conditions

One of the best ways of analyse the effect of wind is to raise a problem of a cruise phase. In this third introductory problem, in order to introduce not only wind but also 3D concepts, it has been considered a 3D climb phase from point ($\lambda = -2.5^0$, $\theta = 41.8^0$, $h = 13123.4\ ft$) to point ($\lambda = 2.45^0$, $\theta = 43.6^0$, $h = 32808.4\ ft$). The initial mass has been set to $m = 51200\ kg$ and the rest of boundary conditions have been left free.

Wind model used has been the one used for the case of study and applied in paper [11]. The wind forecast considered correspond to 20 October 2010 at 38,612 ft in the European region following the model described in Section 4.3.1. The polynomial approximation is valid for an area covering Western Europe, longitude $\lambda \in [-5, 14]$ degrees and latitude $\theta \in [40, 53]$ degrees.

The surfaces obtained in the regression and shown in Figure 6.2 are polynomials which are functions of the latitude and longitude.

The trajectory obtained for both wind and no-wind solutions are shown in Figure 5.5. Wind is also plotted in subfigure (b) for the region around the initial and final points.

Wind model is considered only as function of the locating coordinates, this is, the altitude profile is not directly conditioned by wind. However, it is affected indirectly because wind changes the velocity profile. Note that the altitude curve is similar to previous introductory problem. In addition, since boundary conditions for χ have been set free, the no-wind solution is a VM, i.e. a motion contained in a vertical plane with $\chi = const.$

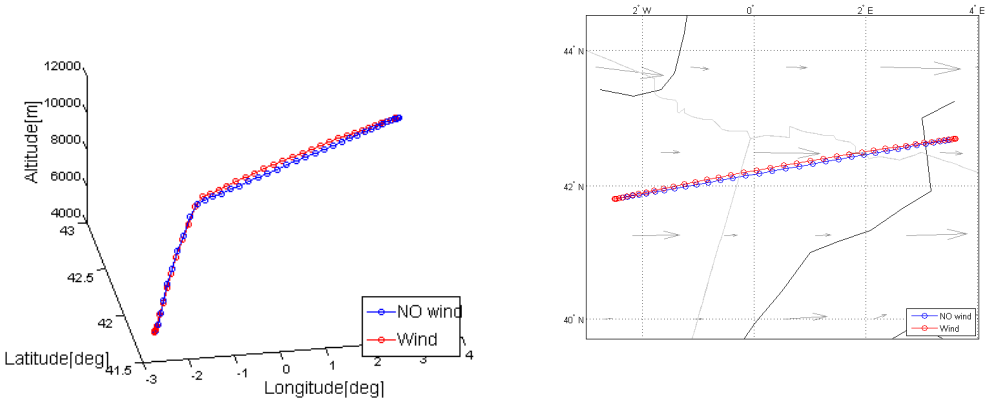

(a) 3D trajectory

(b) 2D trajectory

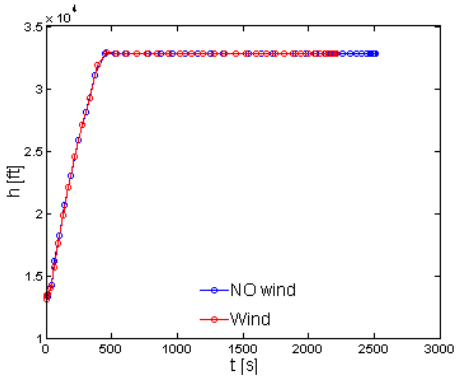

(c) Altitude vs. time

Figure 5.5: *Trajectory of 3D climb wind effect analysis problem*

The equations of motion governing this 3D motion are Equations 4.1. and have a relevant importance:

$$\dot{x} = V\cos(\gamma)\cos(\chi) + w_x \tag{4.1a}$$

$$\dot{y} = V\cos(\gamma)\sin(\chi) + w_y \tag{4.1b}$$

which define the ground velocity components, $\dot{x}$ and $\dot{y}$, as the sum of TAS velocity, v, corrected for γ and χ plus the wind velocity w_x and w_y. For the conditions this problem is dealing with, the wing, if decomposed in the direction of v, has positive sign (wind in the direction of the trajectory). In addition it has also a positive crosswind component.

The results obtained for the states are shown in Figure 5.8 and the corresponding to the controls in Figure 5.7.

Paying attention to the 2D trajectory, the no-wind model takes the straight line between initial and final points as the optimal flight, i.e. the shortest line. However, wind conditions move to trajectory to take a slightly curvilinear path to North. The wind effect ends up with a faster and a more optimal flight in terms of fuel saving. For 40 nodes the fuel burned for both conditions is:

No wind conditions	Fuel consumption = 1417.07 kg
Wind conditions	Fuel consumption = 1245.29 kg

The physical reasons of the solution are described below. As introduced, and looking at Equations 4.1a and 4.1b, for this particular problem, wind is a positive contribution to ground velocity. This means that for the same ground velocity, $\dot{x}$ and $\dot{y}$, if tailwind, the aerodynamic velocity v is smaller.

Since drag is directly proportional to v, positive w_{wind} (tailwind) is favourable in terms of fuel saving.

In order to understand more easily the fuel saving due to tailwind, consider only the constant altitude part of the flight. The fuel consumption is a function the thrust which must equal drag force. Since lift equals weight, the required thrust curve (Figure 5.6) is defined by Equation 5.1:

$$Thr = Drag = \frac{1}{2}\rho S V^2 C_{D_0} + \frac{4C_{D_i}(mg)^2}{\rho S V^2} \tag{5.1}$$

Curve has a double contribution. Up to the minimum, the contribution given by the effect of induced drag is higher. Then, the effect of velocity is predominant.

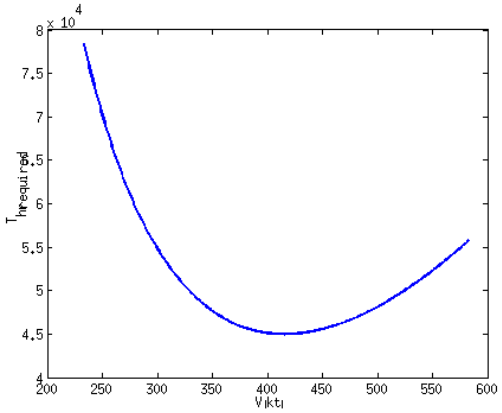

Figure 5.6: *Thr_{req} for a cruise vs. v*

The aircraft is flying in the right side of the curve (higher velocities) where a grater velocity gives a higher drag and thus a greater thrust is required. Tailwind reduces aerodynamic velocity v for the same ground velocity ($\dot{x}$ and $\dot{y}$) optimizing fuel.

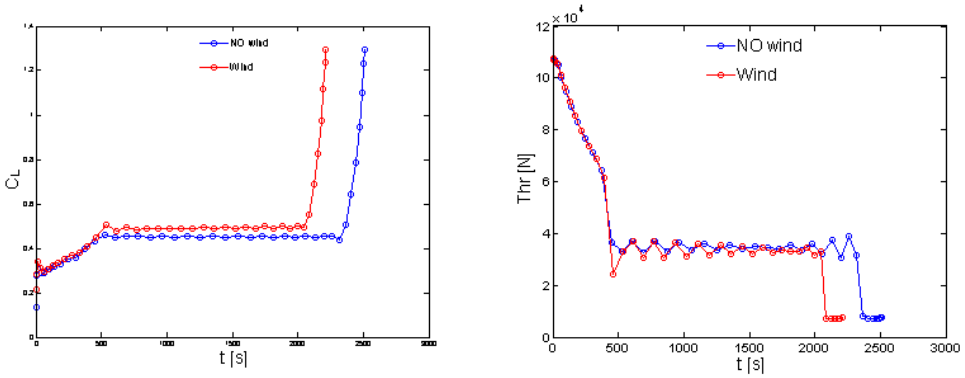

(a) C_L vs. time (b) Thr vs. time

Figure 5.7: *States of 3D climb wind effect analysis problem*

The effect on the velocity and mass can be noticed in Figure 5.8(a) and 5.8(c). Below, the results obtained for the flight path, heading and bank angles are displayed. γ follows the expected result, with and initial positive angle, 0 at cruise and negative at descent section. It must be also noticed the results obtained for χ and μ which are adjusted to get the optimal curvature of the trajectory.

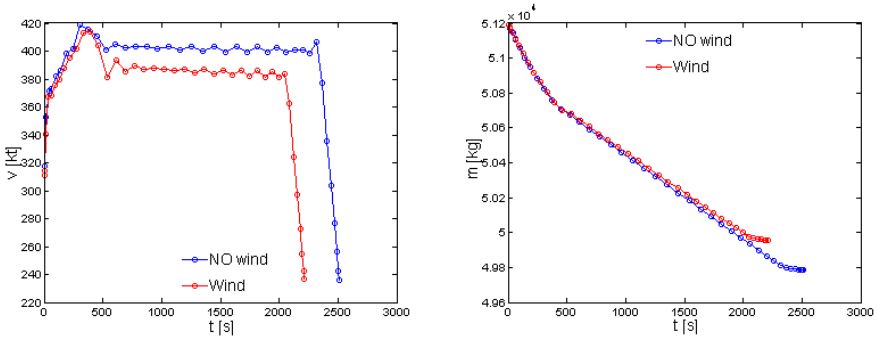

(a) v vs. time

(b) m vs. time

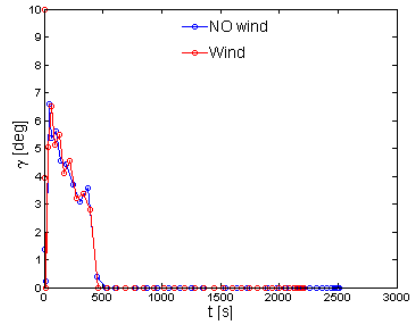

(c) γ vs. time

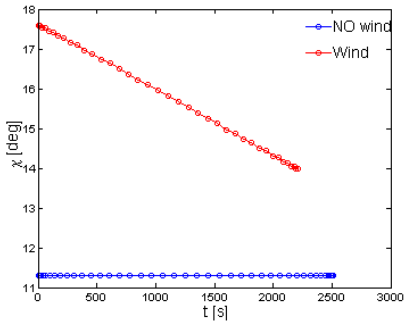

(d) χ vs. time

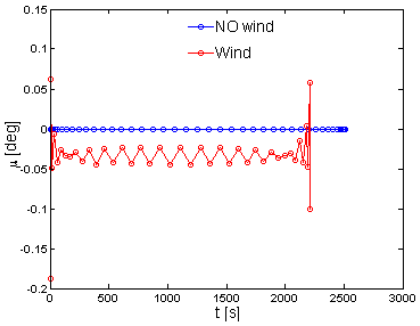

(e) μ vs. time

Figure 5.8: *Controls of 3D climb wind effect analysis problem*

Chapter 6

Case study

6.1 Introduction

The objective of the case study is to solve a complete optimization problem of a realistic commercial flight. The route chosen is a flight from Madrid Barajas (LEMD) to Berlin Schöenefeld (EDDB).

As it has been already introduced, the problem is the case of study solved in [11] by mean of Hermite-Simpson method. In this case, the numerical method used has been Legendre pseudospectral method. The problem follows the flight plan described in the following sections and aims to obtain the minimum mass of fuel necessary to cover the route subjected to the real elements involved in a commercial flight as the air traffic management (ATM) procedures, wind, etc.

6.2 Problem setup

The goal of this section is to explain the flight plan faced, and the way in which the model has been transformed into an optimal control problem.

The problem is build as a multiphase optimal control problem. Each phase is modelled in concordance with different conditions described below. The problem division in phases is part of the nature of the model since it is it is required in order to include the restrictions of the model. These constraints are related to the aerodynamic configuration (AC), atmosphere model (AM), etc. but also on the departure and landing procedures, waypoints and operation altitudes.

Flight plan

Departure from Madrid Barajas is modelled as PINAR1AU SID procedure from runway 15L. The Departure point is at altitude $h_i = 2034\ ft$ and has coordinates $\lambda = -3.56\ deg$, $\theta = 40.47\ deg$.

The definition of this particular SID procedure can be found in the Aeronautical Information Publications (AIP) Spain, published by Aeropuertos Espaoles y Navegacin Area (AENA): *To MD034 on heading* 144 *deg (Magnetic North) at* 2600 *ft or above, turn left. To MD035 at* 5700 *ft or above, turn left. To RBO at* 13000 *ft or above, turn right. To PINAR at* 13000 *ft or above.* The coordinates of the different waypoints and navigational aids are:

- MD034 (aRea NAVigation (RNAV)): 40 deg 26'37.3164" N; 003 deg 30'21.236" W;
- MD035 (RNAV): 40 deg 21'30.9920" N; 3 deg 19052.545000 W;
- RBO (VOR/ DME): 40 deg 51'14" N; 3 deg 14'47" W;
- PINAR (RNAV): 40 deg 58'49.0620" N; 2 deg 35'56.9980" W.

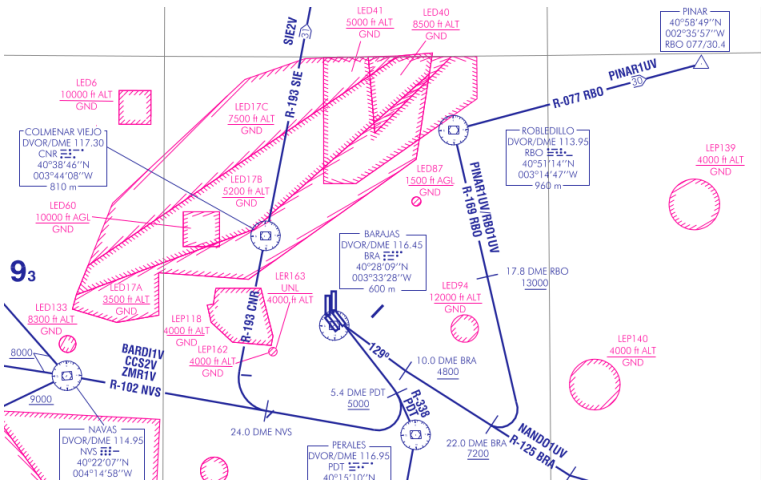

Figure 6.1: *SID PINAR (Source: AIP AENA)*

Take off and initial climb trajectory has been fixed by mean of a constant heading angle $\chi = -54\ deg$ corresponding to the runway direction and a constant flight path angle $\gamma = 4.5\ deg$ introduced as part of the IC procedure and to get a smooth climb. Before cruising, flight plan specifies a cruise leg

at FL360. After that, a step climb is considered to reach the optimal cruising altitude. This altitude is one of the optimality variables that the problem must determine.

Landing in Berlin Schöenefeld is expected to be on runway identified as 25L. Its location is at altitude $h_f = 160\ ft$ and coordinates $\lambda = -13.52\ deg$, $\theta = 52.38\ deg$. In the approach and landing phases, the heading angle has been also constrained to face the runway in the correct direction: $\chi = 25\ deg$. The flight path angle has been restricted to be constant but free in order the problem to compute the optimal approaching γ.

Aircraft

As introduced previously, the aircraft modelled has been an Airbus A-320 following BADA 3.9 [6]. The model is fully described in Section 4.4 and the particular information regarding aircraft A320 for the BADA model is collected in ANNEX I.

Objective

In general, when airlines build their business trajectories, the function to minimize is the so-called cost index (CI). The CI is a function that takes not only into account the fuel, but also includes time and costs that arise from them: $CI = \frac{Time\ cost\ [\$/hr]}{Fuel\ costs\ [cents/lb]}$.

Considering that this analysis cannot take into account the cost of time or fuel, the parameter chosen to be minimized has been the fuel consumed along the whole flight. For this reason, it has been considered that the aircraft reaches the destination with the minimum fuel but without using the reserves. The landing weight (LW) can be then defined as:

$$LW = OEW + PL + RF = 58000\ kg$$

where OEW stands for operating empty weight, PL for payload and RF for reserve fuel. The optimization problem will give then as result the mass of fuel that must be load. It must be noticed that fuel reserves must be added to the problem and cannot be added to the final result in order to be coherent. This is due to the fact that if the aircraft flights with more mass, the performance changes completely giving different values of the decision variables, states and controls.

Phases

Taking into account the problem definition, the flight has been divided into 17 different phases. Below it has been described the particular characteristics of each one. In order to clarify the section, Table 6.1 has been introduced with the aircraft aerodynamic configuration (AC), the atmosphere model (AM) that can be either below (Be) or above (Ab) the tropopause, and other operational and more concrete restrictions. The changing time between phases is a free parameter that will give the optimum flight.

$\mathbf{n_{Phase}}$	**Name**	**DM**	**AC**	**AM**	**OP**	**Details**
1	Take off	VM	TO	Be	$V_{CAS} < 250\ kt$ T_{max}	$\chi = -54\ deg$ $\gamma = 4.5\ deg$
2	Initial Climb	VM	IC	Be	$V_{CAS} < 250\ kt$ T_{max}	$\chi = -54\ deg$ $\gamma = 4.5\ deg$
3	SID 1	3D	CR	Be	$V_{CAS} < 250\ kt$ T_{max}	—
4	SID 2	3D	CR	Be	$V_{CAS} < 250\ kt$	—
5	SID 3	3D	CR	Be	$V_{CAS} < 250\ kt$	—
6	SID 4	3D	CR	Be	—	—
7	SID 5	HM	CR	Be	—	$h = 13000\ ft$
8	Vertical climb	VM	CR	Be	—	—
9	First cruise	HM	CR	Ab	—	$h = 36000\ ft$ $t > 120\ s$
10	Free step	3D	CR	Ab	—	—
11	Second cruise	HM	CR	Ab	—	$h = free$
12	Free descent	3D	CR	Ab	—	—
13	Vertical descent	VM	CR	Be	—	—
14	Deceleration	HM	CR	Be	$V_{CAS} < 250\ kt$	$h = 10000\ ft$
15	Free descend	3D	CR	Be	$V_{CAS} < 250\ kt$ T_{min}	—
16	Approach	VM	AP	Be	$V_{CAS} < 250\ kt$	$\chi = 25\ deg$
17	Landing	VM	LD	Be	$V_{CAS} < 250\ kt$	$\chi = 25\ deg$

Table 6.1: *Case study: Phases*

First seven phases follow the departure flight plan (SID) described in previous paragraphs. Take off and initial climb are produced aligned with the runway and at constant rate of climb (ROC). SID procedure leads to 5 different phases in order to overflight the waypoints and altitude checkpoints collected in Table 6.2. In addition, also operative conditions in terms of maximum throttle has been fixed to phases 1 to 3.

Phases 8 to 10 describe the climb up to cruise altitude. This climb includes a change of atmosphere model (crossing tropopause) and including a cruise leg at 36000 ft. This cruising leg is opposite to optimality conditions and the problem will try to neglect it joining phases 8 and 10. For this reason, a constraint has been added fixing a minimum time of duration for this phase of 2 minutes.

In phase 11, which, as introduced, is maybe the main phase, the aircraft cruises at the optimal constant altitude. This altitude is one of the main results contained in the decision vector.

The descending segment is formed by phases 12 to 17 including approach and landing phases at constant but free flight path angle and fixed heading angle aligned with the arrival runway. The descend includes the change in the atmosphere model and also a deceleration phase at constant altitude at 10000 ft (Phase 14).

Boundary conditions

In Table 6.2, the boundary conditions and interphase restrictions are collected. It must be taken into account that in addition to what included in the table, initial time has been set to 0: $t_i = 0\ s$, leaving free the time at which the change of phase is produced. The initial velocity is set to the minimum allowed $V = 151.7\ kt$ and the final mass to 58000 kg as explained above.

The beginning of the approaching phase has been considered at 6000 ft over the arrival runway altitude and the landing phase at 2000 ft over that altitude.

It must be noticed that due to the multiphase model character, it has been added the linking constraints on the states for the interphase nodes. This follows what explained in Section 2.2.

BC	Name	Lon [deg]	Lat [deg]	h [ft]	Details
Initial	LEMD	-3.56	40.47	2034	Initial conditions
1 – 2	TO → IC	—	—	—	Change in AC
2 – 3	IC → CR	—	—	—	Change in AC
3 – 4	MDO34	-3.50359	40.4395	—	—
4 – 5	MDO35	-3.32542	40.3531	—	—
5 – 6	h_{10000}	—	—	10000	—
6 – 7	RBO	-3.24639	40.8539	13000	—
7 – 8	PINAR	-2.59917	40.9803	13000	—
8 – 9	h_{Trop}	—	—	36000	—
9 – 10	—	—	—	36000	—
10 – 11	—	—	—	—	—
11 – 12	—	—	—	—	—
12 – 13	h_{Trop}	—	—	36000	—
13 – 14	—	—	—	1000	—
14 – 15	—	—	—	1000	—
15 – 16	CR → AP	—	—	6160	Change in AC
16 – 17	AP → LD	—	—	2160	Change in AC
Final	EDDB	-13.52	52.38	160	Final conditions

Table 6.2: *Case study: Boundary conditions*

Wind approximation

Wind mathematical model was introduced in Section 4.3.1 and applied in the third introductory problem. It applies a polynomial regression for an specific forecast set of points. In particular 20 October 2010 at 38,612 ft in the European region weather forecast has been used.

The polynomial approximation is valid for an area covering Western Europe, longitude $\lambda \in [-5, 14]$ degrees and latitude $\theta \in [40, 53]$ degrees and can be represented by the surfaces $w_x = f(\lambda, \theta)$ and $w_y = f(\lambda, \theta)$ which are functions of the longitude and the latitude.

Wind effects has been only applied on phases 9 to 14 and neglected in the rest of phases for the sake of simplicity, since they cover the biggest proportion of the flight.

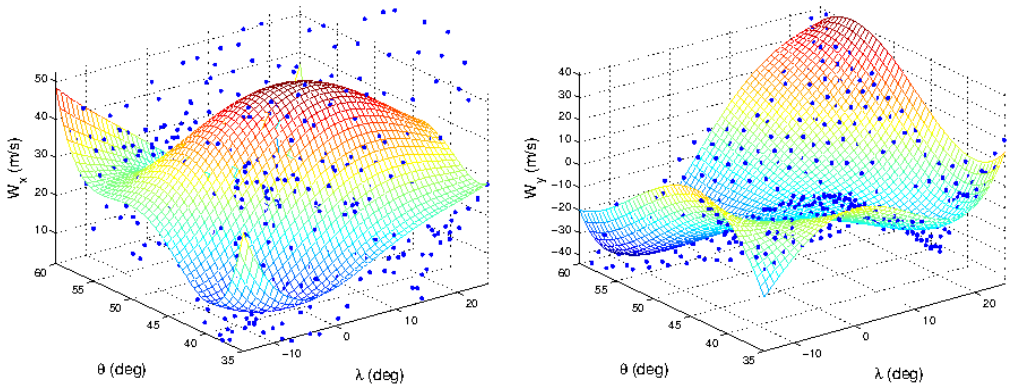

(a) Wind in x direction (b) Wind in y direction

Figure 6.2: *Wind model*

Numerical considerations

Notice that the problem has been formulated as a multiphase optimal control problem and Pseudospectral method has been applied for the discretization of the equations of motion transcribing the infinite-dimensional problem into a finite-dimensional one.

Regarding the length and importance of the phases, the nodes has been distributed in order to guarantee a good result. This is, it has been applied a greater number of grid points in phases that require it. In addition it has been checked the efficiency of the method by using different number of collocation points. It must be mentioned that it has been used the same initial guess approximation even for the changing number of nodes.

The problem has been written using AMPL language and the resulting NLP problem has been solved using IPOPT, which showed robustness in solving infeasible subproblems in the iterative process, even when dealing with infeasible initial guesses. The computer used has been a personal laptop with an Intel© Core^{TM} i7-2630QM processor and 4GB of RAM.

6.3 Results

The optimal solution obtained for the flight is presented below. In order to introduce the optimal flight, in Figure 6.3 it has been shown a first general view the optimal trajectory to the flight plan described from Madrid Barajas

to Berlin Schöenefeld airport. In the subfigure (a), the 3D trajectory is shown with its ground projection (in grey). This ground projection has been displayed in subfigure (b) with the wind map of the region affecting.

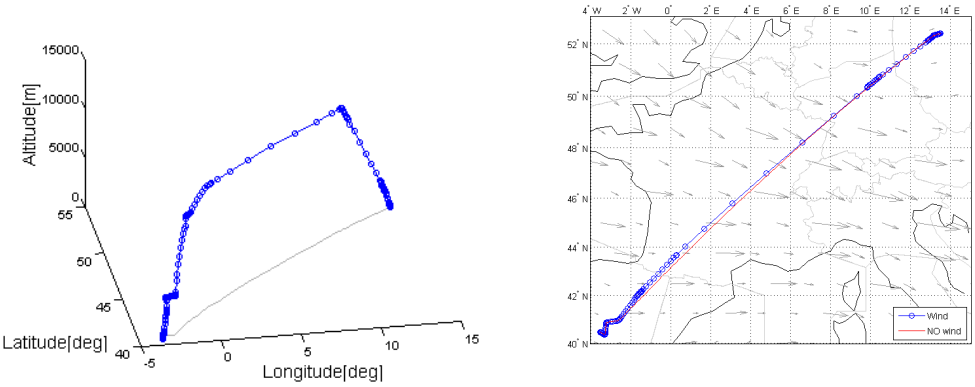

(a) *3D trajectory* (b) *Trajectory ground projection*

Figure 6.3: *Optimal trajectory*

The results and graphs collected in this chapter for the states, controls, etc. correspond to the following distribution of nodes:

$$N^{Pn} = 8 \quad \text{for } n = 1, 2, 3, 4, 5, 6, 7, 9, 11, 13, 14, 16, 17$$
$$N^{Pn} = 12 \quad \text{for } n = 8, 10, 12, 15$$

It has been obtained a minimum initial mass of the aircraft of 62578.94 kg which means a fuel consumption of:

Fuel consumtion : 4578.94 kg

The fuel consumption obtained for different distributions of the number of nodes is found in Table 6.4 with the aim of analysing some results regarding the numerical approach.

The numerical values of the optimal trajectory for the nodes distribution already mentioned has been collected in Table 6.3. Switching times and the mass at the end of each trajectory segment, in addition to important results for some states have been presented.

The main results obtained that deserve a special comment are the corresponding to vertical and horizontal phases in which the altitude and orientation have not been fixed for the problem to find their optimal values.

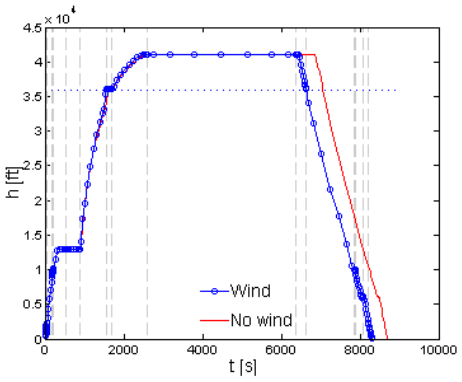

Figure 6.4: *Altitude h vs time*

It should be noticed that the phases described as vertical motion (VM) correspond to segments of the flight in which the displacement of the aircraft is restricted to be in a vertical plane with a determined orientation χ. Optimal values obtained for vertical motion phases number 8 and 13, in which optimal χ values must be determined by the problem, have been: $\chi^{p_8} = 57.2\ deg$ and $\chi^{p_{13}} = 58.4\ deg$. Other important value is the obtained for the in the last two phases of the flight. The runway approach the orientation $\chi^{p_{16}} = \chi^{p_{17}} = 25\ deg$ was fixed, but the approaching angle was left free obtaining an optimal value of $\gamma^{p_{16}} = \gamma^{p_{17}} = -4.64\ deg$.

Even these values are important results, the most relevant result for the optimal flight planning is the cruise altitude corresponding to phase 11. This corresponds to the longest phase and also to the highest fuel consumption. The optimal cruise altitude is $h^{p_{11}} = 41000\ ft$. Figure 6.4 shows the altitude profile along the flight time.

Note that the cruise altitude is a single arc given by the maximum altitude $h_{max} = 41000\ ft$ and Mach number $M_{max} = 0.82$. The optimal altitude and velocity are grater to what the aircraft can withstand. Hence, maximum altitude and Mach restrictions apply. Figure 6.5(d) shows the Mach number vs. time. It must be also noticed that the cruise altitude obtained correspond in this case to a flight level of FL410, because it coincidentally match to the maximum. However, it could have been any altitude in the range. In order words, the coincidence of the optimal cruise altitude with a flight level is anecdotal because the problem do not consider flight levels restrictions. Notice that flight levels are spaced 2000 ft height and can be even or odd: $FL340$, $FL360$, $FL380$ and $FL400$ or $FL350$, $FL370$, $FL390$ and $FL410$.

$\mathbf{n_{Phase}}$	$\mathbf{t_f^{Pn}}$ $[s]$	$\mathbf{m_f^{Pn}}$ $[kg]$	**Optimal states**
1	19.7	62576	Path
2	19.7	62576	Path
3	51.4	62517.3	—
4	184.6	62292.2	—
5	205.0	62265	—
6	542.5	62013.6	—
7	899.4	61730.2	—
8	1563.8	61039.1	$\chi = 57.2\ deg$
9	1683.8	60954.5	—
10	2581.3	60365.6	—
11	6358.3	58228.2	$h = 41000\ ft$ $M = M_{max}$
12	6632.0	58201.3	—
13	7855.3	58062	$\chi = 58.4\ deg$
14	7874.5	58059.5	—
15	8086.4	58030.4	—
16	8220.6	58011.3	$\gamma = -4.64\ deg$
17	8297.2	58000	$\gamma = -4.64\ deg$

Table 6.3: *Case study: results for the optimal trajectory*

As it can be checked, the altitude profile has a similar shape to what was obtained for the second introductory problem in which it was optimized a 2D flight. In no operational procedures were considered, the aircraft would follow a climb with a progressive change in the heading angle up to a cruise phase, and then, it would start to lose altitude suddenly with almost constant descending angle. Despite, due to procedures, it can be noticed that phase 7 determines a cruise phase at 13000 ft before the departure procedure ends at PINAR waypoints. In addition it must be also noticed that a cruise phase was introduced with phase 9 at 36000 ft. It must be noticed that this phase is not efficient because it brakes the climbing curve. It was added a fixed duration of the phase in order the problem not to suppress it.

Regarding the cruise phase, in this case, since optimal values are over the maximum possible for altitude and velocity, the speed does not decrease during cruise phase while fuel is burnt as expected and remains constant at the maximum velocity allowed for the maximum Mach and altitude: $v = v_{h_{max},M_{max}}$.

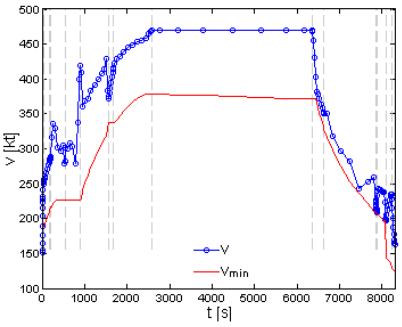

(a) v vs. time

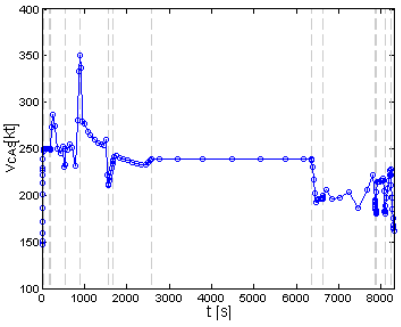

(b) v_{CAS} vs. time

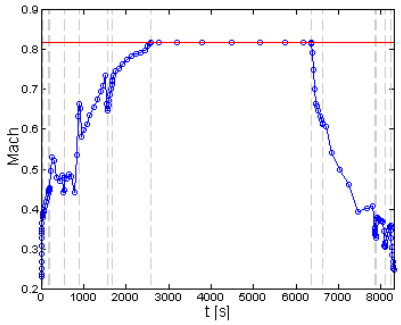

(c) Mach vs. time

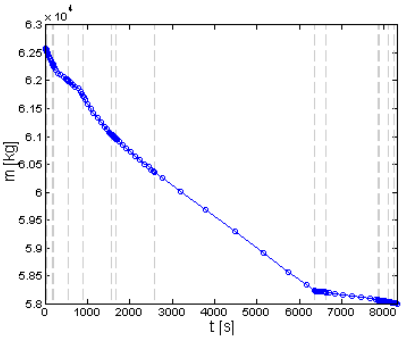

(d) m vs. time

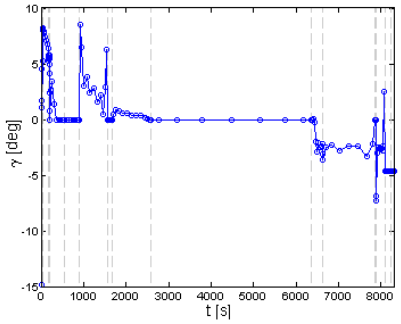

(e) γ vs. time

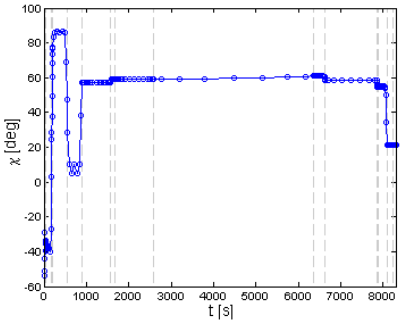

(f) χ vs. time

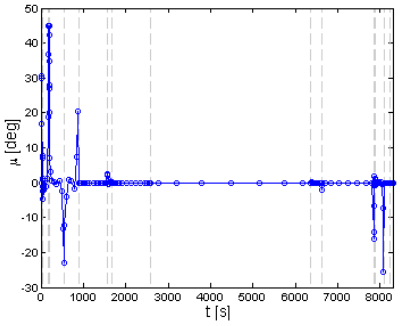

(g) μ vs. time

Figure 6.5: *Case study: states results for the optimal trajectory*

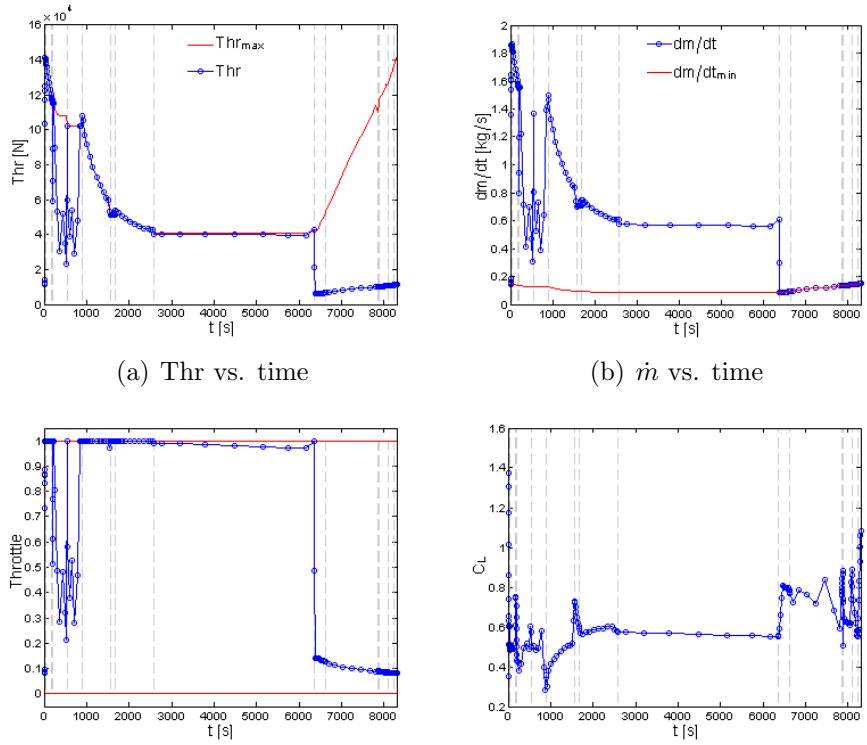

(a) Thr vs. time

(b) $\dot{m}$ vs. time

(c) Throttle vs. time

(d) C_L vs. time

Figure 6.6: *Case study: controls results for the optimal trajectory*

In general, except from the SID manoeuvres, the optimal flight rely on a maximum throttle ascend. Cruise is given at slightly descending throttle and then it turns to the minimum possible giving by the minimum fuel flow. Optimal lift coefficient in first phases takes changing values. but in general, increases up to cruise are reached. Then it starts decreasing very slowly, and during descend, it increases at lower velocities. These results are shown in Figure 6.6.

It must be mentioned again the effect of wind, which is similar to the results obtained in the third introductory problem. The result obtained for the same approach but removing the effect of wind is shown in Figures 6.3(b) and 6.4 which show two main results. The tailwind is favourable in terms of fuel consumption and in addition reduces the time of arrival. Furthermore, it is shown how the path moves slightly in the ground projection to find the optimality trajectory while the altitude profile is similar.

From the mathematical point of view, it can be noticed once again that the order of magnitude of the states affect to the error and the deviations. Note that greater fluctuations are found for the angles, Mach number and C_L.

For the number of nodes used, some interesting information must be mentioned to have an idea of the magnitude of the problem. The written in AMPL (containing more than 2400 net lines) defines a NLP problem of the form described in the introduction of Chapter 3 with the following variables and constraints:

Total number of variables = 1485
Total number of equality constraints = 1223
Total number of inequality constraints = 1618

Table 6.4 collects the results obtained for different number of nodes. It follows the same distribution and it has been named *Phases group A* to phases 1, 2, 3, 4, 5, 6, 7, 9, 11, 13, 14, 16 and 17, and *Phases group B* to phases 8, 10, 12 an 15.

Phases group A nodes	**Phases group B nodes**	**Total number of nodes**	**Consume [Kg]**	**Iterations**	**Solving time [s]**
5	8	97	4647.65	444	10.21
6	10	118	4600.6	359	10.66
8	10	144	4586.48	337	13.40
8	12	152	4578.94	439	18.84

Table 6.4: *Study regarding the number of nodes*

It must be mentioned that the solver is not able to solve the problem with a greater number of grid points. The results show a decreasing error when increasing the number of nodes. However, the solution is far from the precision that can be obtained for simple cases. Despite of the fact that the accuracy of the solution could be poor from the mathematical point of view, from the engineering point of view, the order of magnitude of the error in comparison with the total mass of the aircraft is small. This lets affirm, that it could be use in a real case. In addition, an important result is the fast convergence: solving time lower than 20 s for more than 150 nodes, which opens an interesting field of study to develop.

Chapter 7

Conclusions

Optimization of commercial flights is an important topic that may carry relevant improvements not only in the economical field but also reducing environmental impact.

Current air traffic management system rely on airways, waypoints and flight altitude levels to guarantee safe operations. This system does not provide a great flexibility for optimization, however, the future of air traffic is expected to evolve to a freer scheme in which airlines, owners of the routes, can define the trajectories in agreement with the air traffic authorities.

The systems used currently to determine the flight plan is sometimes not very precise and far from optimality. The definition of the optimization of the flight plan as an optimal control problem provides a complete approach that lets compute all the states (altitude, velocities, C_L and throttle controls, attitude angles, etc.) providing a 4D (time and space) optimization.

This method allows computing, prior to flight, the most suitable path for fuel, time or cost index optimization, getting the complete so-called business trajectory, i.e. the path that better matches the airline interests.

Therefore, regarding the trajectory optimization in the airlines business, it can be concluded that it has a useful but limited application to the current system that will take a greater importance in the near future with the evolution to the new air space paradigm.

This project has focused on the realistic application of optimal control theories for the resolution of the commercial flights optimization problem.

For this task, it has been studied the modelling of the flight plan applying these theories, the solving methods and the existing software to get satisfactory solutions. Specially, regarding the solving methods, it has been studied the application of Legendre pseudospectral method for the equations of motion discretization to obtain the numerical results.

One of the main concussions that has been got is that it is possible to obtain satisfactory solutions with full physical meaning using these techniques. In fact, part of the analysis of the obtained results has focused in the understanding of the optimal performance. Moreover, it has been also analysed the results obtained from the mathematical point of view. The use of Legendre pseudospectral method to discretize the DAE systme has been not an easy task for such a large problem.

Despite there exist very robust specific software as IPOPT (the solver used) to compute iteratively the solutions, some problems have been found. It is known that the pseudospectral methods have an exponential rate of convergence and it has been found that rapidly when increasing the number of nodes, it takes excessive time to get a solution and in some cases, the solver is not able to find it. Despite of this, it must be mentioned that the results show that even that it is not possible to obtain a very precise value for the minimum fuel, the pattern that follows the solution when increasing the number of nodes lets conclude that the results obtained are enough close to the exact solution to be used in real flights. Note that the error is very far from the order of magnitude of the mass of the aircraft.

With the aim of improving and continuing the development it could be considered some guidelines for future work. Regarding the efficiency of the code, it can be studied the way to improve it by an exhaustive debugging of the code (in this case written in AMPL) by removing some unused variables and constrains. It can be also studied the distribution of nodes for the different phases.

From a more engineering point of view, one of the lines of study could go in the direction of the comparison of the Legendre pseudospectral method with respect to other approaches as the Hermite-Simpson which has been wider used in flight optimization. A deepest analysis of the Legendre pseudospectral application could develop the use of this technique more extensively and get benefit of the particular characteristics of the method as the great rate of convergence.

Appendix A

Aircraft data

General information

Symbol	Value	Description
n_{eng}	2	Number of engynes
Engine type	J	Either Jet, Turboprop or Piston
Wake category	H	Either J, H, M or L

Aircraft type block

Symbol	Value	Description
m_{ref}	64 t	Reference mass
m_{min}	39 t	Minimum mass
m_{max}	77 t	Maximum mass
m_{pyld}	21.5 t	Maximum payload mass

Mass block

Symbol	Value	Description
V_{M0}	350 kn (CAS)	Maximum operating speed
M_{M0}	0.82	Maximum operating Mach number
h_{M0}	33295 ft	Maximum operating altitude
h_{max}	41000 ft	Maximum altitude at MTOW and ISA
G_w	432.5 ft/kg	Weight gradient on maximum altitude
G_t	-313.6 ft/K	Temperature gradient on max. altitude

Aerodynamics block

Symbol	Value	Description
S	122.6 m^2	Reference wing surface area
$C_{D0,TO}$	0.033	parasitic drag coefficient (take-off)
$C_{D_{i,TO}}$	0.041	induced drag coefficient (take-off)
$C_{D0,IC}$	0.023	parasitic drag coefficient (initial climb)
$C_{D_{i,IC}}$	0.044	induced drag coefficient (initial climb)
$C_{D0,CR}$	0.026659	parasitic drag coefficient (cruise)
$C_{D_{i,CR}}$	0.038726	induced drag coefficient (cruise)
$C_{D0,AP}$	0.038	parasitic drag coefficient (approach)
$C_{D_{i,AP}}$	0.0419	induced drag coefficient (approach)
$C_{D0,LD}$	0.096	parasitic drag coefficient (landing)
$C_{D_{i,LD}}$	0.0371	induced drag coefficient (landing)
$C_{D0,\Delta LDG}$	-	parasite drag coef. (landing gear)
$V_{stallTO}$	112.1 kn (CAS)	Stall speed TO
$V_{stallIC}$	118 kn (CAS)	Stall speed
$V_{stallCR}$	140.5 kn (CAS)	Stall speed
$V_{stallAP}$	105.1kn (CAS)	Stall speed
$V_{stallLD}$	101.3 kn (CAS)	Stall speed
$C_Lbo_{(M=0)}$	1.4041	Buffet onset lift coef. (jet only)
K	0.79242	Buffeting gradient (jet only)

Engine thrust block

Symbol	Value	Description
$C_{Tc,1}$	142310 N	1st max. climb thrust coefficient
$C_{Tc,2}$	51680 ft	2nd max climb thrust coefficient
$C_{Tc,3}$	5.6809E-11 ft^2	3rd max. climb thrust coefficient
$C_{Tc,4}$	10.138 K	1st thrust temperature coefficient
$C_{Tc,5}$	0.008871 1/K	2nd thrust temperature coefficient
$C_{Tdes,low}$	0.10847	low altitude descent thrust coefficient
$C_{Tdes,high}$	0.13603	high altitude descent thrust coefficient
$H_{p,des}$	29831 ft	transition altitude for calculation of descend thrust
$C_{Tdess,app}$	0.15749	approach thrust coefficient
$C_{Tdess,ld}$	0.39566	landing thrust coefficient
$V_{des,ref}$	310 kn	reference descent speed (CAS)
$M_{des,ref}$	0.78	reference descent Mach number

Fuel flow block

Symbol	Value	Description
C_{f1}	0.75882 $\frac{kg}{minkN}$	1st thrust specific fuel consumption coefficient
C_{f2}	2938.5 kn	2nd thrust specific fuel consumption coefficient
C_{f3}	8.9418 kg/min	1st descent fuel flow coefficient
C_{f4}	93865.0 ft	2nd descent fuel flow coefficient
C_{fcr}	0.96358	cruise fuel flow correction coefficient

Ground movement block

Symbol	Value	Description
TOL	2190 m	take-off length
LDL	1440 m	landing length
span	34.1 m	wingspan
length	37.57 m	length

Bibliography

[1] Becerra, V. M., *Optimal Control and Applications*. Second AstroNet-II Training School. 5-6 June 2013.

[2] Bellman, R. E., *Dynamic Programming*. Priceston University Press, Prieton NJ, 1975.

[3] Betts, J.T., *Practical Methods for Optimal Control and Estimation Using Nonlinear Programming*. Advances in Design and Control. Society for Industrial and Applied Mathematics, 2010.

[4] Bryson, A. E. and Ho, Y., *Applied Optimal Control*. Wiley, 1975.

[5] Canuto, C., *Spectral methods: Fundamentals in single domains*. Springer Verlag, 2006.

[6] Eurocontrol, *User manual for the base of aircraft data (BADA)*. Revision 3.9, 2007.
http://www.eurocontrol.int/services/bada/

[7] Fourer, R., Kernighan, B. W., *AMPL: A Modeling Language for Mathematical Programming*. Duxbury Press, 2002.
http://ampl.com/

[8] Garca-Heras, J., Soler, M. and Sez F. J., *Comparative Analysis of direct Collocation Methods to Aircraft Minimum Fuel Trajectory Problems with Required Time of Arrival*.

[9] Pontryagin, L., Boltyanskii, V., Gamkrelidze, R., and Mishchenko, E., *The Mathematical Theory of Optimal Processes*. Interscience Publishers, 1962.

[10] Soler, M., *Commercial Aircraft Trajectory Planning based on Multiphase Mixed-Integer Optimal Control*. Ph.D. thesis, Universidad Rey Juan Carlos, 2013.

[11] Soler, M., Olivares, A., and Staffetti, E., *Multiphase Optimal Control Framework for Commercial Aircraft Four-Dimensional Flight-Planning Problems*. Journal of Aircraft, 52(1), 274-286. (2014)

[12] Trefethen, L. N., *Spectral Methods in MATLAB*. Philadelphia, PA: SIAM, 2000.